APPLIED HELICOPTER AEROELASTICS
- MODELLING AND TESTING -

H. Strehlow, D. Teves, G. Polz
Eurocopter Deutschland GmbH
München, Germany

Abstract

Helicopter aeroelasticity must address many unique, highly complex and interrelated problems in the fields of dynamics and aerodynamics. Recent research activities and actual problems of applied helicopter aeroelastics are presented with emphasis on modelling and testing.

Rotor aerodynamics benefits tremendously from the rapid growth in the capabilities of computational fluid dynamics. Applications in the development of advanced airfoils and the layout of blade shapes are presented in some detail, including recent wind tunnel test results.

Project-orientated aeroelastic stability and response analysis is based on comprehensive aeromechanical codes for modelling both aerodynamics and structural dynamics of the complete rotorcraft. A key problem in the design and development of modern systems is the aeromechanical stability of hingeless and bearingless rotors; examples are derived from actual flight test. The prediction of vibratory rotor loads using proven rotor wake modelling techniques is covered. Advanced topics of rotor stall flutter and tail rotor stall induced flap-lag-torsional instability are presented, using data from various development activities.

A field of increasing importance in helicopter aeroelasticity is interactional aerodynamics in conjunction with flow induced vibrations. The helicopter tail shake phenomenon belongs to this category. Some explanations for this peculiar problem are discussed and means for successful tail shake suppression are described.

From the realm of rotor servo-aeroelasticity, research activities concerning the individual blade control concept and related techniques are presented, based on recent wind tunnel and flight test experience.

1. Introduction

The important role of aeroelasticity in the design and development of modern helicopters is fully recognised by the research and manufacturer's community. In the broadest sense, helicopter aeroelasticity encompasses all stability and response problems including the various aerodynamic interference effects. Obviously the complexity of rotary wing aeroelastic problems is partly attributed to the complicated aerodynamic environment of the helicopter, shown in Fig.1 (from Ref.1 with minor modifications).

Therefore all rotors of modern helicopters suffer from the adverse aerodynamic environment at high speeds or load factors. In addition to the periodic change from transonic speeds at the advancing blade to high lift conditions at low Mach numbers at the retreating blade, interference effects from the fuselage induced flow field, the rotor wake and the unsteady flow emanating from the rotor hub-pylon-engine (cowling) may have strong impact on the tail surfaces, the tail rotor, and the airframe.

Thus the complexity of helicopter aeroelastic problems is readily explained by the numerous interaction and coupling effects, many of them being inherently nonlinear or related to timevariant periodic coefficients. Therefore the modelling and solution of rotorcraft aeroelastic problems is a difficult task and requires adequate aerodynamic and structural dynamic models for the various elements listed in Fig.2. The key for a successful comprehensive aeroelastic analysis in the helicopter industry is a consistent, balanced choice of appropriate models and solution methods. At Eurocopter Deutschland (ECD) aeroelastic predictions rely on the CAMRAD codes (Ref.2, 3), EC's helicopter code HOST (Ref.4) and various special purpose codes developed inhouse.

The aerodynamic models include a free wake representation of the rotor inflow as well as a nonlinear description of the blade section aerodynamics, based on Mach number dependent airfoil characteristics. Blade sweep, yawed flow, and dynamic stall effects are taken into account by appropriate empirical corrections. The structural dynamic models include an elastic representation of the rotor blade deformations. For many problems the modelling of the "vibration chain" fuselage, control system, drive train is required, too. Adequate structural dynamic models are based on a hybrid multibody algorithm using the finite element method, a modal representation or a rigid body approach, see Ref.5.

In the following sections, recent research activities and actual problems of applied helicopter aeroelastics at ECD are presented with emphasis on modelling and testing.

2. Helicopter Rotor Aerodynamics - Recent Research Studies

Advances in rotor aerodynamics, allowing improvements in helicopter performance, and expansion of the overall flight envelope are an important topic in industrial research. Rotor aerodynamics benefits tremendously from the rapid growth in the capabilities of computational fluid dynamics (CFD), see Ref.6.

Airfoil Development for Rotor Blades

As mentioned already, rotor blades are operating in a highly varying aerodynamic environment. Three specific regions can be identified for a rotor airfoil, see Fig.3 (left), defining the airfoil performance requirements:

1. For the advancing blade, the required lift coefficient is very low at high advance ratios. Because of the limited lift capability of the retreating blade a high drag rise Mach number is desired.
2. At the for and aft rotor position at moderate Mach numbers (which are decisive for hover conditions as well), lift coefficients of $c_L = 0.6$ are typical over nearly the whole blade span. Obviously, a high lift-to-drag ratio is required at these operational conditions for good rotor performance in both hover and forward flight.
3. At the retreating blade, high lift coefficients at low Mach numbers are required especially at high advance ratios. Thus the maximum lift coefficient at the retreating blade should be as high as possible.
4. Finally, it is vital that the airfoil pitching moment level should be limited at all occuring angles of attack to minimise both torsional blade deflections and rotor control loads.

It is obvious from this assessment that some of the goals are difficult to meet or even contradictory. More details on the general problem of rotor blade airfoil design are found in Ref.6,7. The design objectives are shown in Fig.3 (right) for two airfoils which are used for different radial blade positions.

Lower Mach numbers at the inner blade sections allow relatively thick airfoils with high lift capability (favourable for the retreating blade), whereas the high Mach numbers in the tip region require thinner airfoils with low transonic drag and thus less lift capability.

The results of a modern rotor blade airfoil development at ECD and DLR are shown in Fig.4, demonstrating the benefits of the DM-H4/H3 airfoils relative to the "classic" NACA 23012 airfoil. The DM-H4 airfoil with 12% thickness is designed for inner blade sections, whereas the 9% thick DM-H3 airfoil is fitted to the transonic flow conditions at the blade tip. The airfoils were tested in the Transonic Wind Tunnel Braunschweig of the DLR, see Ref.8.

Advanced Geometry Blades and Tips

Rotor blade planform and tip shape optimisation is another significant area of advanced rotor design activities. In recent years many attempts were made to develop appropriate 3D-shapes for the blade tip suitable for main rotor applications. Modern CFD-methods are very helpful for studying the pros and cons of different blade tip designs. In Fig.5 the local Mach number distributions over the upper blade surface are plotted at the transonic flow conditions of an advancing blade for three different tip designs:

- Rectangular, NACA 23012 airfoil
- Tapered, DM-H4/H3 airfoils
- Parabolic, DM-H4/H3 airfoils

Obviously, for these flow conditions the conventional rectangular blade is inferior in comparison to blades with advanced tip shapes and modern airfoils. The numerical results were obtained by an Euler-code modified to simulate non-constant inflow over radius (Ref.9). The blade tip design problem is specially addressed in Ref.10.

An overview of the geometry of various main rotor blades developed at ECD during the last twenty-five years is presented in Fig.6. With the exception of the BO105 and the similar BK117 blades, all blades are equipped with the new DM-H4/H3 airfoil family. The blades with tapered tip are favourable in hover and at level flight speeds common for todays flying helicopters. They are successfully applied now as "upgrade" for both the civil and the military versions of the BO105 helicopter. A power reduction of more than 10% was measured with the new blades in high altitude and at higher flight speeds (Ref.11). For the EC135, the serial production version of the BO108, blades with parabolic tip were selected, similar to the Tiger blade tip design. In addition the German/ Indian project ALH is fitted also with similar blades. Parabolic tips seem to be favourable at high speeds and load factors, typically required for modern helicopter projects.

High Speed Rotor Blade Research

In order to further improve and exploit the maximum speed range of helicopters, special research activities are launched at industry, see Ref.12. At Eurocopter, research on new blades with unconventional shape, twist and tip design was carried out recently in the joined ORPHEE program of ECF and ECD, see Fig.7. In order to shift the operational limits of the rotor to even higher flight speeds, the lift capability of the retreating blade is enlarged for two blade designs by using negative taper. All blades are fitted with airfoils of the OA3 series which show similar aerodynamic characteristics as the DM-H4/H3 airfoils. The outer tip shapes of the tested blade sets have a parabolic leading edge and an anhedral bent down tip for keeping away the blade tip vortices from the following blades. Parameters for the optimisation were the lift-to-drag ratio L/D at 350km/h and the steady lift capability C_T/σ at 150km/h. Model rotor wind-tunnel tests (Modane, DNW) confirmed the expected performance benefits of the EC3 and EC4 blades, whereas the test results for the nonlinear twisted EC2 blade are not convincing.

As a typical result of the aeroelastic behaviour, Fig.8 shows the measured and calculated radial distribution of vibratory 3/rev flap-bending blade moments for the EC1 reference blade. The correlation between calculation and test is excellent in this case ($\mu = 0.1$, $C_T/\sigma = 0.075$).

3. Helicopter Aeroelastic Stability and Response - Selected Problems

Project-orientated aeroelastic stability and response analysis in helicopter industry is based on so-called comprehensive aeromechanical codes. These codes are capable to model the aerodynamics and dynamics of different rotorcraft configurations by proven technology - often with good results. The following sections are aimed to present a limited number of actual aeroelastic problems of modern helicopters with emphasis on modelling and testing.

3.1 Helicopter Aeromechanical Stability

A key problem in the design and development of modern rotor systems is the aeromechanical stability.

Dynamic Rotor Lay-Out

Helicopter rotors are usually classified according to the mechanical arrangement of the hub design to accommodate the blade flap and lead-lag motion, see Fig.9:

- The articulated rotor with conventional flap, lead lag and pitch hinges
- The so-called hingeless rotor with removed flap and lead-lag hinges
- The bearingless rotor with all three hinges removed.

From the aeroelastic point-of-view, the appropriate selection of the fundamental flap and lead-lag blade natural frequencies determines the aeromechanical stability characteristics of the rotor and the helicopter system. Typical design ranges for various rotor systems are indicated in Fig.9. The dynamic layout of ECD's main and tail rotors are shown, too. Obviously the so-called soft inplane hingeless and bearingless main rotor systems and the stiff inplane tail rotors of the see-saw and bearingless types are forwarded and used in ECD's current helicopter projects. The rationale for this decision is discussed in Ref.13, 14.

Inplane Rotor Damping

Soft inplane hingeless and bearingless main rotor systems are selected for modern helicopters in order to control the blade stresses. But these systems are susceptible to a coupled rotor-body aeromechanical instability, called air and ground resonance. Before going into details, Fig.10 shows the design of ECD's hingeless and bearingless main rotors:

- Hingeless rotors of BO105 and BK117 with titanium hub, conventional pitch bearings and inplane blade friction damping
- Hingeless rotors of Tiger and ALH with composite or "integrated" hub respectively, elastomeric pitch bearing and inplane fluid damper
- Bearingless rotor of EC135 (BO108) with titanium hub/shaft, pitch control by torque tube and flexbeam, and inplane elastomeric damper

All rotor systems have composite blades with "tailored" flapwise and inplane bending stiffness in the blade neck or flexbeam area. A key item in soft inplane rotor design is the provision of adequate lead-lag blade damping for eliminating air and ground resonance problems. All systems are equipped with efficient means for providing high blade inplane damping values, see Ref.13 to 16.

Pitch-Lead Coupling

In order to further improve and augment the blade inplane damping, aeroelastic bending-torsion coupling is an appropriate means. The measured and calculated inplane modal damping and natural frequency data of Fig.11 for the hingeless BO105 and the bearingless EC135 rotors clearly demonstrate the favourable damping increase at high rotor thrust. This effect is well known in rotor aeroelasticity and attributed to the stabilizing effect of negative blade pitch-lead coupling for soft inplane rotors:

- Hingeless rotor blades with "unmatched" bending stiffness data in the neck area produce negative torsional inputs by nonlinear bending for the leading blade at high thrust conditions.
- Bearingless rotors with a specific blade pitch control geometry introduce a favourable negative pitch-lead coupling at high rotor thrust operational conditions.

Air Resonance

The development of soft inplane hingeless and bearingless rotors has generated considerable research on air and ground resonance in the past. The aeromechanical stability margin depends on the damping of the blade inplane motion and of the coupled body (fuselage) system modes.

The following discussion concentrates on the air resonance phenomenon, which is strongly influenced by aerodynamic dampings. In the frequency diagram of Fig.12 the potential "resonances" are indicated by the near coalescence of the natural frequencies of either the body pitch and roll modes and of the frequency of the inplane (regressive) rotor "driving" mode in the nonrotating system. For typical hingeless and bearingless rotors only the body roll mode is within the airborne rotor operational speed limits and thus of practical importance. This case is found for instance at the upgraded BO105 CBS-5 helicopter, where potential air resonance may be encountered near nominal rotor speeds. It should be noted that the frequency curves of the BO105 CBS-5 are derived for the inplane rotor mode and the body modes "separately" without aerodynamics, using multi-blade coordinates. The rotor inplane regressive mode is a circular mode, which generates a rotating unbalance at the hub. The body modes depend mainly on the flapping stiffness of rotor blades and the aircraft inertia data. Both modes are generated by coupling the aircraft with either the longitudinal or the lateral regressive flapping mode.

The coupled rotor-body frequency and damping behaviour in the vicinity of the nominal rotor rotational speed at air resonance are plotted in detail in Fig.13 for the undamped case. The inplane auto-excitation of the hub would "drive" the aircraft unstable. But due to both rotor inplane and body-roll damping the helicopter is actually stable, see Fig.13, below. This result is elaborated for the 60 kts level flight case, for which appropriate test data are available. The stabilising effect of aerodynamics is associated mainly with the high body damping (from rotor flapping) and partly with the stabilizing effect of negative pitch-lead coupling which is typical for the hingeless BO105 rotor system. Therefore the inclusion of aerodynamics in any air resonance stability analysis of hingeless and bearingless rotors becomes indispensable, see Ref.17, 18.

3.2 Vibratory Rotor Loads and Response

Accurate prediction of rotor loads and rotorcraft vibration has been a challenge to helicopter aeroelasticians in the past and still remains a difficult and often intractable problem.

Rotor Wake Modelling

The correlation of predicted and measured 3/rev vibratory shaft bending moments (rotating system) in Fig.14 clearly demonstrates the need of an adequate rotor wake model which is of special importance in transition flight and at low level flight speeds. All data are taken from the upgraded BO105 CBS-5 helicopter. The analytical model is based on the CAMRAD/JA code. Correct free-flight trim was achieved by iterations on initial control settings until aircraft force and moment equilibrium was reached. The blade modal representation includes elastic flap/lag bending and torsion. The wake geometry of the rotor is prescribed from flow visualisation studies of similar rotors at the same operational conditions, or it is obtained as part of the solution from a free wake calculation, based on Scully's procedure. The blade is represented by a lifting line and the wake is modelled as a combination of tip vortex and single inboard vortex filament with large core radius. The effect of unsteady shed wake is considered only at the inboard near wake. (Note: The wake plots on the right side of Fig.14 are borrowed from Ref.19 for visualisation purpose.) The best results are obtained for the free wake model, whereas the prescribed wake is appropriate only in high speed flight. As expected, the simple uniform inflow model is not sufficient for vibratory rotor load prediction. Similar results were obtained in Ref.20.

Therefore free wake methods which allow the wake vorticity field to evolve in free motion, are the basis for successful vibration predictions. As pointed out in Ref.21, there is a need to further improve current free wake models and to reduce substantially the computer time, if free wake methods are accepted as common tools in helicopter aeroelasticity. In cooperation with the University of Stuttgart, an unsteady 3D vortex-lattice method with a free wake vortex model for rotor downwash representation is under development, see Ref.22, 23. Impressive free wake simulations are presented in Fig.15, showing the vortices emanating from one blade under forward flight conditions. The rotor wake varies continously and is influenced by rotor-fuselage interferences. These effects contribute to the unsteady inflow of the rotor blades. The studies are carried out for the 4-bladed model rotor (2-Meter Rotor Test System) of NASA Langley, see Ref.24. The calculated and measured induced velocity distributions of the rotor disk are in remarkably good agreement.

Helicopter Vibrations

Almost without exception, vibrations have been a problem for all helicopters, and vibrations will continue to play an important role in the development of the next generation of helicopters, see Ref.25. With a helicopter in forward flight, the non-uniform flow passes the rotor and causes oscillating airloads on the rotor blades which produce excitation forces and moments at the rotating hub. This moves the helicopter vibration problem to the realm of aeroelasticity. The hub excitations are almost perfectly periodic in steady flight. The predicted and measured shaft bending moments (time histories) at three different level flight speeds are presented in Fig.16 for the BO108 helicopter (predecessor of EC135) using the CAMRAD/JA code with its free wake modelling capability. These moments are associated with the rotating system. The correlation between calculation and flight test is quite good.

The bearingless rotor concept with redundant load paths (flexbeam and control cuff) requires advanced modelling effort. Using the finite element modelling capabilities of the CAMRAD II code, the load transfer of the EC135 bearingless rotor was studied in some detail. Typical results are presented in Fig.17 showing the spanwise 3/rev blade flap bending moment distribution at 32 kts level flight. Despite the limited number of available, strain gauges it can be concluded that the predictions correspond well with the flight test data.

The periodic rotor loads are transmitted from the rotating hub system to the fixed airframe system, acting as so-called blade-number-harmonics which are multiples of the blade passing frequency $n\Omega$. This frequency is determined by the number of blades n and the rotational frequency Ω of the main rotor. Using these fixed system hub forces and moments as excitations in a structural dynamic finite element fuselage model, vibration predictions are possible with some success. The 4Ω vertical vibrations at the pilot of the EC135 prototype with a 4-bladed bearingless rotor system are calculated by this method. The results are presented in Fig.18 for level flight conditions. The comparison with flight test results is satisfactory. It should be noted that current helicopters have to rely still on some means of vibration control for reducing the vibration levels to acceptable values of 0.1g at the first blade-number-harmonic. Reducing the rotor hub excitations by aeroelastic means is a challenge for future research activities.

3.3 Main Rotor Stall Flutter

A general design objective of rotorcraft manufacturers is a helicopter that has both high manoeuvre and high forward speed capability. Obviously, these flight cases show high angles of attack at the retreating blades. Hence, dynamic stall effects are of fundamental importance.

Dynamic Stall

The dynamic stall occurs on helicopter rotor blades experiencing unsteady motion. Dynamic stall results in a "stall delay" with angles of attack beyond the static-stall angles, see Fig.19 (left side, taken from Ref.26). This phenomenon leads to a beneficial dynamic lift overshoot, accompanied by a hysteresis pitch moment characteristic, which may result in negative pitch damping. These nonlinear unsteady effects depend primarily on the reduced frequency and the sign of the pitch motion, but also on the airfoil type and the Mach number. An unsolved problem in helicopter applications is the need for a time domain stall model, which is valid not only for single harmonic angle of attack variations, but also for non-harmonic and even non-periodic motions.

Reliable modelling of dynamic stall effects is of special importance for aeroelastic prediction of both rotor blade and control loads and stability. In the CAMRAD/JA code the dynamic stall representation is based on Gormont's model (Ref.??), which provides a dynamic overshoot and hysteresis pitch moment damping. The calculated angle of attack distribution is plotted in Fig.19 (right) for the BO105 with standard blades (NACA 23012 airfoil) at high forward speed and moderate load factor, showing incidence angles well above 15° at the retreating blade.

More advanced stall models for helicopter rotors are under development, all of which are based on measured airfoil data, see Ref.27 and the literature cited there. Although much progress has been made in recent years, dynamic stall remains a major research problem.

Torsional Blade Excitations

The loading of the pitch links which react on the blade aerodynamic and dynamic pitch moments, usually is one of the main restrictions on helicopter flight envelope. Alternating pitch link loads typically show a rapid increase when blade stall or severe compressibility occurs. With a proper component sizing, the strength and fatigue problem of the pitch links can be solved in practice, but a sharp load rise may be a sign that the rotor is near its aerodynamic limitations. Under extreme operational conditions even aeroelastic stability considerations are of concern.

Typical measured pitch link loads in manoeuvre flight (left turn) are presented in Fig.22. The stall onset is easily identified by a sharp nose down spike at the retreating blade near 200° azimuth position.

Typical torsional excitation sources at the rotating blade are listed below.

Advancing Blade:

- Negative aerodynamic spring effects due to nonlinear bending (see Ref.28)
- Impulsive torsional excitation due to high negative airfoil pitch moments (at transonic operational conditions known as "Mach Tuck", see Ref.29)

Retreating Blade:

- Negative aerodynamic damping due to stall induced pitch moment hysteresis (see Ref.26, 30)

Stall Flutter Induced Pitch Link Loads

Helicopter stall flutter is a consequence of high angles of attack which occur at the retreating blade accompanied by high self-excited pitch link oscillations due to the above mentioned negative pitch moment damping. In order to gain further insight into the mechanism of pitch link load oscillations at deep stall, Fig.21 shows the measured time histories and amplitude spectra of torsionally soft (C-spar) and stiff (D-spar) experimental BO105 rotor blades with trapezoidal tip shape. The limit cycle oscillations - best characterized by the stall flutter spike frequency - are restricted mainly to the third and forth quadrant of the rotor disk. Outside the stall region the blade torsional damping is usually sufficiently high and any transient oscillations are damped out quickly.

Therefore rotor blade stall flutter commonly appears as a rotor-periodic phenomenon and may thus be characterized by the rotor harmonics.

The possibility of non-periodic stall induced pitch link load waveforms depends on the extension of the stall region of the retreating blade and on the aerodynamic environment of the advancing blade. It was demonstrated by high speed flights (see Ref.31) that both nonlinear transonic effects at the advancing blade and dynamic stall effects at the retreating blade may lead to non-periodic aeroelastic blade oscillations. Such oscillations were observed during early testing of torsional stiff blades on the BO105. These flight test data are presented in Fig.21, below. The non-rotor harmonic components are obvious from the corresponding amplitude spectrum. Using advanced digital filtering techniques, the processed flight test data of Fig.21 are presented in Fig.22 (left side) showing the high frequency pitch link oscillations of both the torsional soft (BO105 C/C1) and stiff (BO105 '87) experimental blades. Obviously, the stiff blade spike-frequency is higher than the corresponding frequency of the soft blade.

In a greatly appreciated stall flutter investigation of Boeing Vertol in 1974 (see Ref.32) the effect of blade torsional stiffness was evaluated in detail. The following results were found:

- Stall induced torsional oscillations characterized by the stall flutter spike frequency do not correlate well with the blade torsional frequency.
- Torsionally soft blades may have better stall flutter characteristics than stiffer blades.

ECD's flight test data analysis with different rotor blades seems to support the findings of Ref.32:

- The measured spike frequencies correlate only partly with the blade torsional frequency, see Fig.22 (right).
- The measured nondimensionalized pitch link load "amplitudes" - corresponding to the stall flutter oscillations with the spike frequency - are more favourable for the torsional soft C-spar blades, see Fig.23. (Note: In Ref.33 similar pitch link load amplitudes were found in flight tests.)

The flight test data of Fig.23 indicate that a reduction of torsional blade moments and pitch link loads may be achieved using aerodynamic stabilisation by

- special blade swept-back tip design for a slight rearward shift of the blade aerodynamic center and
- sufficient "life twist" by relatively low torsional blade stiffness design.

Finally, measured rotor stall flutter boundaries of conventional rectangular blades (NACA 23012) are compared with new advanced geometry blades (DM-H4/H3) in Fig.24. It can be concluded that modern rotor blades with new thin airfoils at the tips do not suffer from reduced C_T/σ vs. μ limits. In the past thin airfoils showed a detrimental effect with respect to stall flutter, see Ref.31.

3.4 Tail Rotor Stall Induced Flap-Lag-Torsional Instability

Tail rotors are usually of stiff inplane type for reasons of robustness and vulnerability. These rotors are free from aeromechanical stability restrictions, but other aeroelastic blade stability problems are likely to occur for this concept. A detailed overview of ECD's research activities on bearingless tail rotors is given in Ref.34.

Dynamic Lay-Out of a Stiff Inplane Tail Rotor

The 4-bladed stiff inplane bearingless tail rotor (BTR) for the ALH (Advanced Light Helicopter), a cooperation program with Hindustan Aircraft Ltd., is currently flight tested in Bangalore, see Fig.25. It is well known from the literature and confirmed by the ALH aeroelastic analysis that for the stiff inplane concept the fundamental blade bending frequencies in flapwise and edgewise direction should be well separated for adequate aeroelastic stability margins with respect to blade flap-lag stability at higher collective settings. The ALH frequency diagram (in vacuum) is shown in Fig.26. With consideration of built-in pitch-flap coupling for limiting blade flapping, the blade tuning of the fundamental bending frequencies remain well separated under all rotor operational conditions. Thus flap-lag stability is of no concern for the ALH bearingless tail rotor.

Stall Induced Limited Cycles

A second potential problem is the stall induced flap-lag instability at extreme collective angles that is related to the (static) stall characteristics of the airfoil. This phenomenon was first studied in detail for a torsional stiff model rotor in Ref.35. On full-scale tail rotors, this instability phenomenon may be influenced by the torsional dynamics of the rotor blades, too. In the frequency diagram of the ALH (Fig.26), the uncoupled 2nd flap bending and the 1st torsional rotor modes are "crossing" the 3/rev-excitation frequency slightly above the nominal rotor speed. These modes are of interest for the stall induced flap-lag-torsional stability behaviour of the ALH-BTR.

The thrust potential of the ALH-BTR is presented in Fig.27 (left). According to whirl tower measurements, the rotor thrust did not increase beyond pitch angles of 24° (at 0.7 radius) due to stall effects. This is confirmed by the theoretical analysis of Fig.27 (right side): The outer parts of the blade encounter the airfoil stall limit at pitch settings below 25°. The

ALH uses the 12% thick S102C airfoil (inboard) and the 8.3% thick S120E airfoil at the tip.

Measured amplitude spectra of the blade bending moments in flap-direction and lead-lag direction (not shown) and of the pitch control forces for different pitch settings are presented in Fig.28. These measurements document the sudden increase of 3/rev-blade bending and control loads at high pitch angles, signalising the beginning of stall induced flap-lag-torsional limit cycle oscillations, see Fig.29 (right). The measured beating phenomenon in the blade bending moments is due to the coalescence of the limit cycle frequency (self-excitation) and the 3/rev rotor harmonic frequency (forced excitation).

The results of a comprehensive aeroelastic stability analysis with flap and lead-lag bending and torsional modal degrees of freedom are presented in Fig.29 (left). The modal dampings are plotted vs. the pitch angle at 0.7 radius. Blade stability deteriorates at high pitch settings which corresponds well with the whirl tower measurements. Any significant influence of the blade torsional dynamics is not predicted by these studies. Therefore it is concluded that the frequency "crossing" - addressed before in Fig.26 - of the 2nd flap-bending natural frequency with the torsional frequency is not decisive for this phenomenon.

3.5 Helicopter Tail Shake

A field of increasing importance in helicopter aeroelasticity is interactional aerodynamics in conjunction with flow induced vibrations. The helicopter tail shake phenomenon belongs to this kind of problems. According to Fig.30, tail shake may be caused or influenced by both the hub-pylon-engine (cowling) wake and the fuselage-aftbody wake. Two different wake effects are to be considered:

- Trailed vortices leading to wake impingements on tail planes, side fin, tail rotor, etc.
- Vortex shedding resulting in fluctuating lateral airframe forces that excite the fundamental lateral aircraft bending mode by the Lock-In phenomenon.

Both effects are discussed in some detail in Ref.36, 37. The influence of periodic vortex shedding on structural dynamics and the Lock-In phenomenon is carefully explained in Ref.38, for example. In Fig.31, the key effects of vortex shedding on a 2D cylinder are gathered for convenience. The periodic wake of a smooth circular cylinder depends on the Reynolds number. Discrete turbulent vortex shedding is observed at a typical Strouhal number of 0.2 and Reynolds numbers greater than 3.5×10^6. The Lock-In phenomenon is observed if the cylinder is elastically supported . If the flow velocity varies so that the shedding frequency approaches the natural frequency of the cylinder, the vortex shedding suddenly locks into the natural frequency.

Tail Shake Explained by the Lock-In Phenomenon

From the dynamic point of view helicopter tail shake shows a strong resemblance with the Lock-In phenomenon. This subject is further elaborated in Fig.32 using BK117 flight test data. Vortex induced tail boom lateral bending moments are observed at two different frequencies:

- The 1st lateral aircraft bending frequency due to Lock-In effect.
- The vortex shedding frequency in case that Lock-In effect is not "present".

Assuming a Strouhal number of 0.2, a Lock-In region with strong lateral tail boom bending moment excitation by vortex shedding can be identified for the BK117 in a limited flight speed range. For this helicopter, the most severe tail shake is observed at descent flight and flight speeds of 70 to 120kts accompanied by a strong beating phenomenon, see Fig.33.

The time and frequency domain analysis of the flight test data allows a simple interpretation of this beating phenomenon: The nearby bending and shedding frequencies are excited with comparable amplitudes, leading to the annoying beating.

In order to shed more light onto tail shake, "short time" power spectra over a period of 10 secs were processed using different sensor signals:

- Lateral tailboom bending moments and pilot-seat vibrations correlate well, showing strong airframe vibrations during tail shake, see Fig.34.
- Dynamic wake pressure measurements and lateral tail rotor gearbox vibrations do not show any significant wake impingement effects during tail shake, see Fig.35.

Concluding, tail shake can be measured at the airframe as lateral vibrations and on the tailboom as lateral bending moments.

Means for Reducing Tail Shake

For production helicopters tail shake excitations must be reduced to a very low level, so that it is not felt either by crew or by passengers. Thus strong effort is often needed in the development phase of a helicopter in order to reduce tail shake excitations to level of acceptance, usually by aerodynamic means.

Despite the still incomplete understanding of tail shake and the missing of effective prediction methods, there are aerodynamic modifications on the hub (hub cap), on the pylon (fairings) and on the engines (streamlined cowlings) that improve the tail shake behaviour substantially, compare Ref.39, 40. The benefits of a hub cap for reducing BK117 tail shake excitations are demonstrated best by Fig.36 taken from Ref.40. The measured tail boom lateral bending moments are expressed here as peak-to-peak/2-values, which do not correspond to the amplitudes used in Fig.32.

In future, vortex induced helicopter airframe oscillations should be analysed by adequate testing procedures and eventually by advanced CFD-codes in order to gain a more complete understanding of the problem and to derive efficient practical solutions.

4. Helicopter Servo-Aeroelasticity - Current IBC Research Activities

Rotor active control has a broad scope. In the realm of servo-aeroelasticity, ECD's current research activities are concentrated on the development of technologies that may have impact on the expansion of the flight envelope of the next generation of helicopters, see Ref. 41.

Individual Blade Control (IBC)

The introduction of IBC is the most promising active rotor control concept to achieve a major improvement of helicopter performance and comfort. The realisation of IBC by rotating pitch link actuators is forwarded by ZF Luftfahrttechnik in cooperation with Eurocopter Deutschland, see Fig.37. Full scale tests were performed on the BO105 hingeless rotor system both in flight (BO105 S1 helicopter) and in the NASA Ames 40 x 80ft wind tunnel. The IBC-hardware is further described by the system data, collected in Fig.38. The concept uses hydraulic actuators with slip-ring devices for hydraulic power and data transmission through the rotor shaft.

Test Results

Within a joint research program of NASA Ames Research Center, ZF Luftfahrttechnik, DLR and ECD, two wind tunnel test campaigns were performed with a full scale BO105 rotor at NASA Ames, see Ref.42. Main test goals were the acquisition of data with various IBC-inputs for exploring the possibility of rotor power reduction, stall flutter suppression, vibration and noise control etc.

The effect of 2/rev-blade pitch inputs on rotor power at high speeds is shown in Fig.39. The measured 4% power reduction at ±1° inputs is explained mainly due to the more favourable angle of attack distribution in the first quadrant of the rotor disk at the blade tip. Further improvements are to be expected by optimisation of the control inputs.

The potential of IBC with respect to simultaneous vibration and noise reduction was successfully demonstrated by the wind tunnel tests at NASA Ames. At descent flight conditions with strong BVI noise (43 kts speed, +4° shaft tilt) combined 2/rev and 5/rev pitch control inputs with 1,5° and 0.25° respectively, were used resulting in 12 dB noise and 80% vibratory hub load reduction, see Fig.40.

The subject of vibration reduction by IBC was already investigated in flight on the BO105, using pitch actuators with limited authority due to safety reasons. Typical test results at level flight are presented in Fig.41. Depending on the IBC-input phase, 4/rev-cabin vibrations can be significantly reduced by higher harmonic inputs as low as 0.4°. Various aeroelastic calculations with and without IBC pitch inputs were carried out with success, see Ref.43.

Current research acitivities at ECD are concentrating on the implementation of a closed-loop IBC control system on the BO105 helicopter using reactionless 2/rev rotor mode control for BVI reduction and reactive 3/rev, 4/rev, and 5/rev rotor mode control for vibration reduction (compare Ref.41). It is planned to start the BO105 flight tests in 1997.

In the future, rotor servo-aeroelasticity may change dramatically with the introduction of smart materials. Especially for individual blade control, piezoelectric actuation of blade flaps is expected to be a real alternative to the hydraulic pitch actuators, see Ref.44.

5. Conclusion

The review of applied helicopter aeroelastics at ECD is concluded with the following remarks:

- Although many aspects of rotary wing aeroelastics appear similar to fixed wing aeroelastics, the differences are great.
- Helicopter aeroelastics must address many unique, highly complex and interrelated problems in dynamics and aerodynamics.
- Improved understanding of helicopter aeroelastics was achieved by sophisticated comprehensive codes and improved testing methods over the last two decades.
- Nevertheless, current codes have to be further improved in order to solve all aeroelastic problems of today's helicopters.
- There is a chance that in future modern CFD-methods help to accomplish better aeroelastic predictions in helicopter industry.

6. References

1 W.J. Boyne, D.S. Lopez (ed.), **Vertical Flight: The Age of the Helicopter**, Smithsonian Institution Press, Washington, 1984

2 W. Johnson, **Development of a Comprehensive Analysis for Rotorcraft-I, II**, Vertica, Vol.5, 1981

3 W. Johnson, **Technology Drivers in the Development of CAMRAD II**, American Helicopter Society Aeromechanics Specialists

Conference, San Francisco, California January 19-21. 1994

4 G. Arnaud, B. Benoit, F. Toulmay **Améliorations du Modèle Aérodynamique du code rotor hélicoptères R 85 validation et applications,** 28ème Colloque d'Aérodynamique Appliquée I.S.L., France, Oct. 1991

5 H. Strehlow, **An Advanced Rotorcraft Model Using a Hybrid Multibody Algorithm**, Workshop on Dynamics & Aeroelastic Stability Modelling of Rotorcraft Systems, Boca Raton, Florida, Nov. 1987

6 G. Polz, **Current European Rotorcraft Research Activities on Development of Advanced CFD Methods for the Design of Rotor Blades**, 17th European Rotorcraft Forum, Berlin, Germany, Sept. 1991

7 P.F. Yaggy, **Future Rotorcraft Research in the USA**, The Aeronautical Journal of the Royal Aeronautical Society, Vol.73, Sept. 1969

8 K.H. Horstmann, H. Köster, G. Polz, **Improvement of Two Blade Sections for Helicopter Rotors**, 10th European Rotorcraft Forum, The Hague, The Netherlands, Aug. 1984

9 H. Huber, **Rotorcraft Research and Technology Advances at MBB**, 14th Annual General Meeting of the Aeronautical Society of India, Madras, India, Dec. 1988

10 J.J. Philippe, A. Vuillet, **Aerodynamic Design of Advanced Rotors with New Tip Shapes**, 39th Annual Forum of the AHS, St. Louis, Missouri, May 1983

11 D. Braun, A. Humpert, **BO105 CBS-5: BO105 Upgrade Through New Rotor Blades**, 19th European Rotorcraft Forum, Cernobbio, Italy, Sept. 1993

12 A. Vuillet, **The High Speed Helicopter**, 18th European Rotorcraft Forum, Avignon, France, Sept. 1992

13 H. Strehlow, B. Enenkl, **Aeroelastic Design Considerations in the Development of Helicopters**, AGARD Conference Proceedings No.354 on Aeroelastic Considerations in the Preliminary Design of Aircraft, London, United Kingdom, 1983

14 H. Huber, **"Will Rotor Hubs Lose Their Bearings?" - A Survey of Bearingless Main Rotor Development**, 18th European Rotorcraft Forum, Avignon, France, Sept. 1992

15 W. Jonda, J.-P. Libeer, **The France-German Tiger Program: A Status Report**, Vertiflite, Nov./Dec. 1990

16 D. Schimke, B. Enenkl, E. Allramseder, **MBB BO108 Helicopter Ground and Flight Test Evaluation**, 15th European Rotorcraft Forum, Amsterdam, The Netherlands, Sept. 1989

17 R.T. Lytwyn, W. Miao, W. Woitsch, **Airborne and Ground Resonance of Hingeless Rotors**, Journal of the AHS, Vol.16, No.2, April 1971

18 R.A. Ormiston, **Rotor-Fuselage Dynamics of Helicopter Air and Ground Resonance**, Journal of the AHS, Vol.36, No.2, 1991

19 J.D. Berry, D. Hood, J. Elliott, S. Atlhoff, **Helicopter Rotor Induced Velocities Theory and Experiment**, AHS Specialists Meeting on Aerodynamics and Aeroacoustics, Arlington, Texas, Feb. 1987

20 R.M. Heffernan, G. Yamachi, M. Gaubert, W. Johnson, **Hub Loads Analysis of the SA349/2 Helicopter**, Journal of the AHS, Vol.35, No.1, Jan. 1990

21 D. Bliss, W. Miller, **Efficient Free Wake Calculations Using Analytical/Numerical Matching**, Journal of the AHS, Vol.38, No.2, April 1993

22 H. Stahl-Cucinelli, **Vortex-Lattice Free Wake Model for Helicopter Rotor Downwash**, 20th European Rotorcraft Forum, Amsterdam, The Netherlands, Oct. 1994

23 L. Zerle, Final Report of the BRITE/EURAM Project **SCIA (Study and Computation of Interactional Aerodynamics),** Brussels 1992

24 Joe W. Elliot and Susan L. Althoff, **Inflow Measurement made with a Laser Velocimeter on a Helicopter Model in Forward Flight,** (Volume 2), NASA-TM-100542, 1988

25 G. Reichert, H. Strehlow, **Survey of Active and Passive Means to Reduce Rotorcraft Vibrations**, International Symposium on Aeroelasticity, Nuremberg, Germany, Oct. 1981

26 L.W. Carr, **Progress in Analysis and Prediction of Dynamic Stall**, J. Aircraft, Vol.25, No.1, Jan. 1988

27 J.G. Leishman, **Modelling of Subsonic Unsteady Aerodynamics for Rotary Wing Applications**, Journal of the AHS, Vol.35, No.1, Jan. 1990

28 W.F. Paul, R. Zincone, **Advanced Technology Applied to the UH-60A and S-75 Helicopters**, 3rd European Rotorcraft Forum, Aix-En-Provence, France, Sept. 1977

29 R.G. Benson, L. Dodone, R. Gormont, E. Kohler, **Influence of Airfoils on Stall Flutter Boundaries of Articulated Helicopter Rotors**, Journal of the AHS, Jan. 1973

30 W.Z. Stepniewski, C.N. Keys, **Rotary-Wing Aerodynamics**, Dover Publications, New York 1978

31 H. Huber, H. Strehlow, **Hingeless Rotor Dynamics in High Speed Flight**, Vertica, Vol.1, 1976

32 R. Gabel, F. Tarzanin, **Blade Torsional Tuning to Manage Large Amplitude Control Loads**, J. Aircraft, Vol.11, No.8, Aug. 1974

33 J.G. Yen, M. Yuce, **Correlation of Pitch-Link Loads in Deep Stall on Bearingless Rotors**, Journal of the AHS, Vol.37, No.4, Oct. 1992

34 V. Klöppel, H. Huber, B. Enenkl, **Development of Bearingless Tail Rotors**, 16th European Rotorcraft Forum, Glasgow, United Kingdom, Sept. 1990

35 R. Ormiston, W. Bousman, **A Study of Stall-Induced Flap-Lag Instability of Hingeless Rotors**, Journal of the AHS, Jan. 1975

36 H. Huber, G. Polz, **Studies on Blade-To-Blade and Rotor-Fuselage-Tail Interferences**, AGARD Fluid Dynamics Panel Specialists Meeting on Prediction of Aerodynamic Loads on Rotorcraft, London, United Kingdom, May 1982

37 P. Roesch, A.M. Dequin, **Experimental Research on Helicopter Fuselage and Rotor Hub Wake Turbulence**, 39th Annual National Forum of the AHS, St. Louis, Missouri, May 1983

38 R.D. Blevins, **Flow-Induced Vibration**, Van Nostrand Reinhold Company, New York, 1977

39 A. Cassier, R. Wenneckers, J.-M. Pouradier, **Aerodynamic Development of the Tiger Helicopter**, 50th Annual Forum of the AHS, Washington, May 1994

40 H. Huber, T. Masue, **Flight Characteristics Design and Development of the MBB/KHI BK117 Helicopter**, 7th European Rotorcraft and Powered Lift Aircraft Forum, 1981

41 D. Teves, G. Niesl, A. Blaas, S. Jacklin, **The Role of Active Control in Future Rotorcraft**, 21th European Rotorcraft Forum, Saint-Petersburg, Russia, Sept 1995

42 S. Jacklin, A. Blaas, D. Teves, R. Kube, **Reduction of Helicopter BVI Noise, Vibration, and Power Consumption through Individual Blade Control,** American Helicopter Society 51st Annual Forum, Forth Worth, TX, May, 1995.

43 D. Teves, V. Klöppel, P. Richter, **Development of Active Control Technology in the Rotating System, Flight Testing and Theoretical Investigations**, 18th European Rotorcraft Forum, Avignon, France, Sept. 1992

44 H. Strehlow, H. Rapp, **Smart Materials for Helicopter Rotor Active Control**, Smart Structures for Aircraft and Spacecraft, 75th Meeting of the AGARD Structures and Materials Panel, Conference Proceedings 531, Lindau, Germany, Oct. 1992

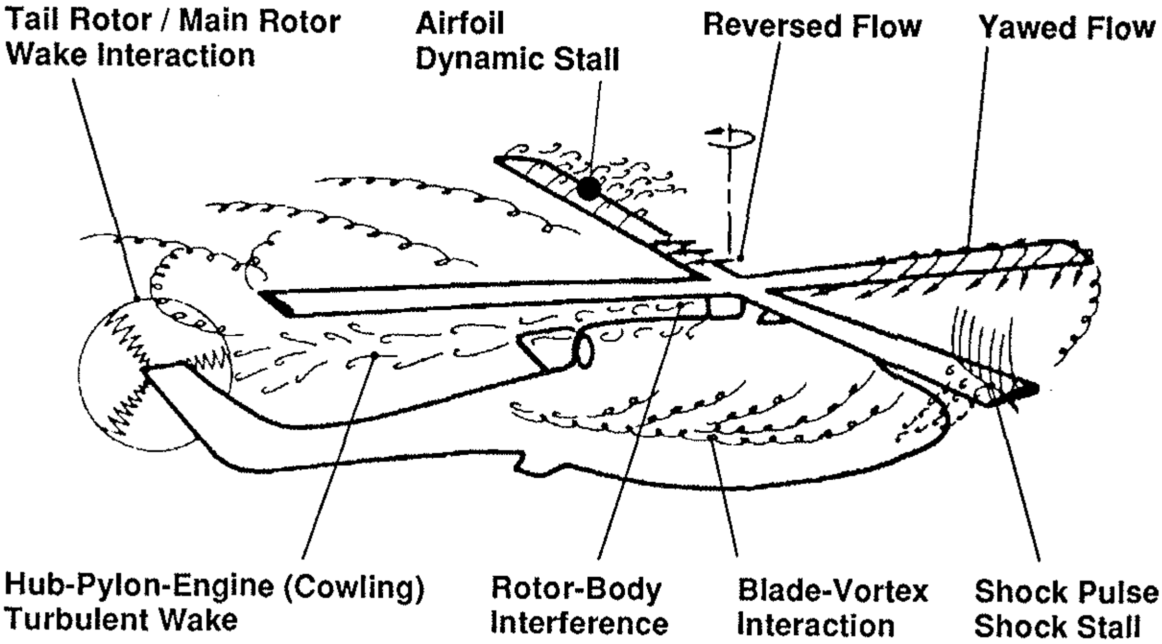

Fig.1: Aerodynamic environment of the helicopter

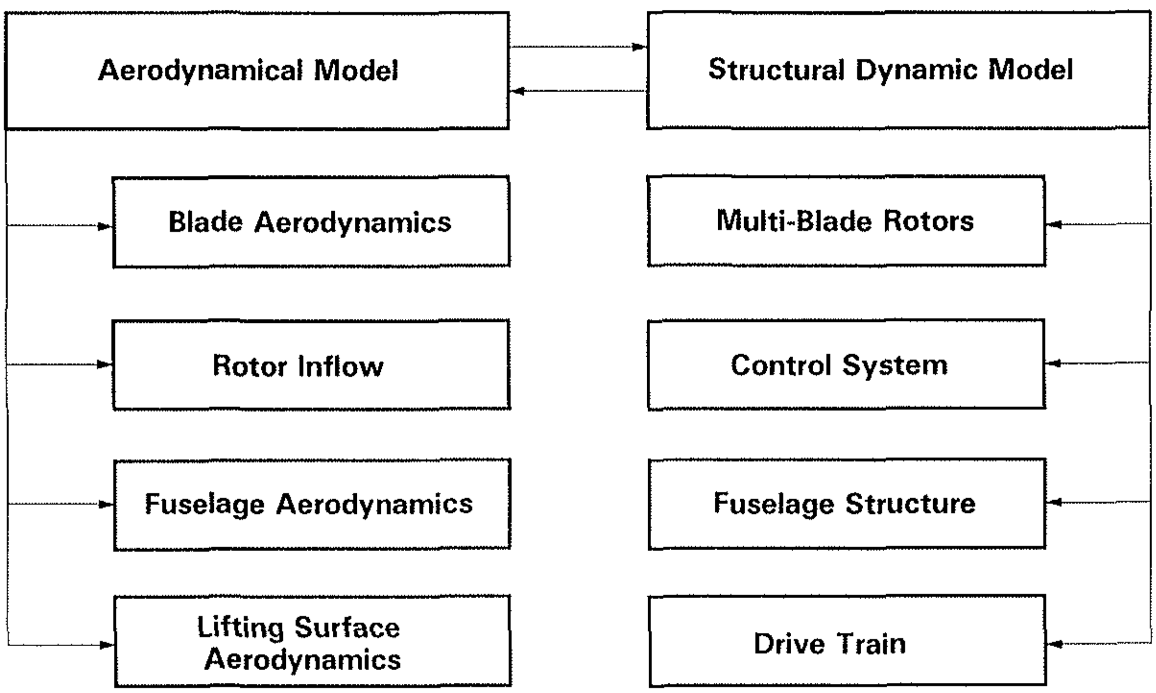

Fig.2: Aeroelastic rotorcraft modeling

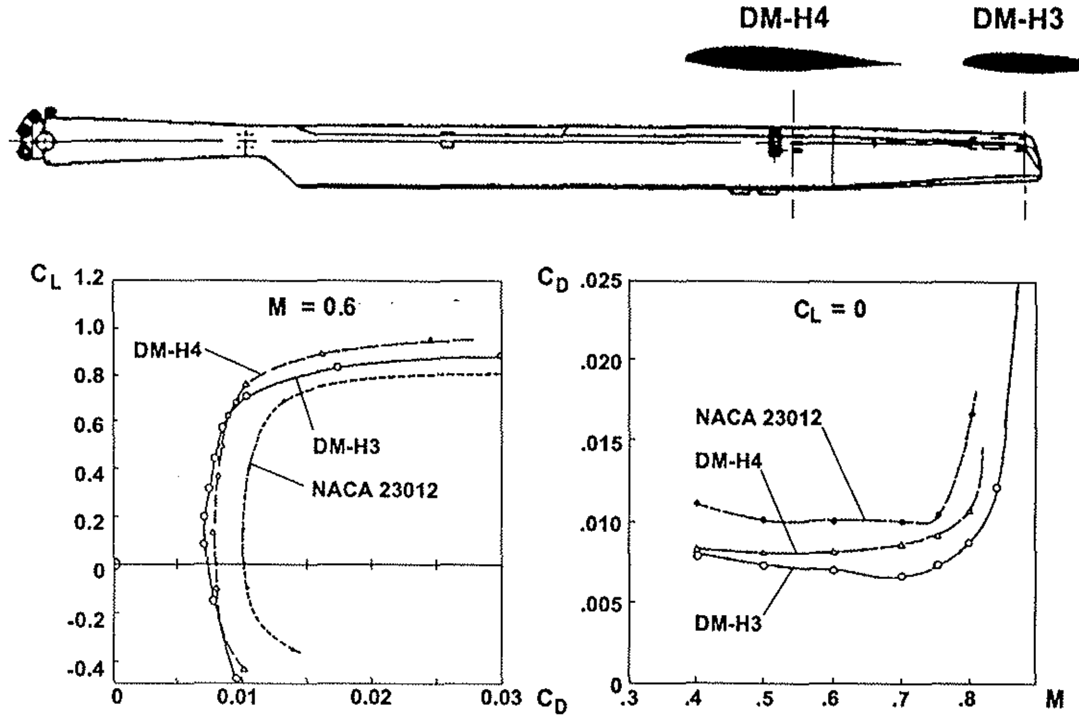

Fig.3: Essential operational conditions and aerodynamic requirements for blade airfoils

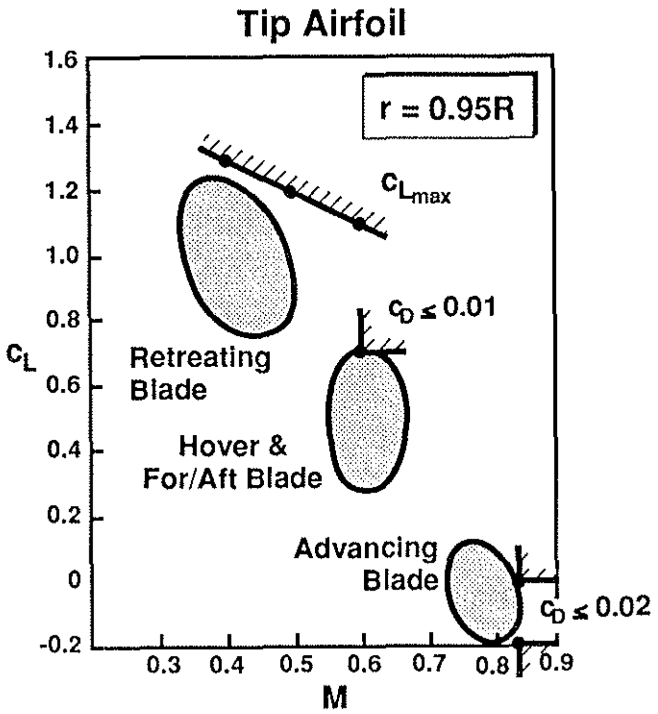

Design Objectives For Two Airfoils

Design objective	Inner airfoil	Tip airfoil
Thickness	12%	9%
Drag divergence ($c_D = 0.02$)	$M > 0.8$ at $c_L = 0/0.2$	$M > 0.84$ at $c_L = -0.2/0$
Drag at $M = 0.6$, $c_L = 0.7$	$c_D \le 0.01$	$c_D \le 0.01$
Maximum lift at $M = 0.3$	$c_{Lmax} = 1.5$	
$M = 0.4$	$c_{Lmax} = 1.4$	$c_{Lmax} = 1.3$
$M = 0.5$	$c_{Lmax} = 1.3$	$c_{Lmax} = 1.2$
Pitching moment below stall inception	$\|c_m\| \le 0.01$	$\|c_m\| \le 0.01$

Fig.4: Modern airfoils for advanced geometry blades

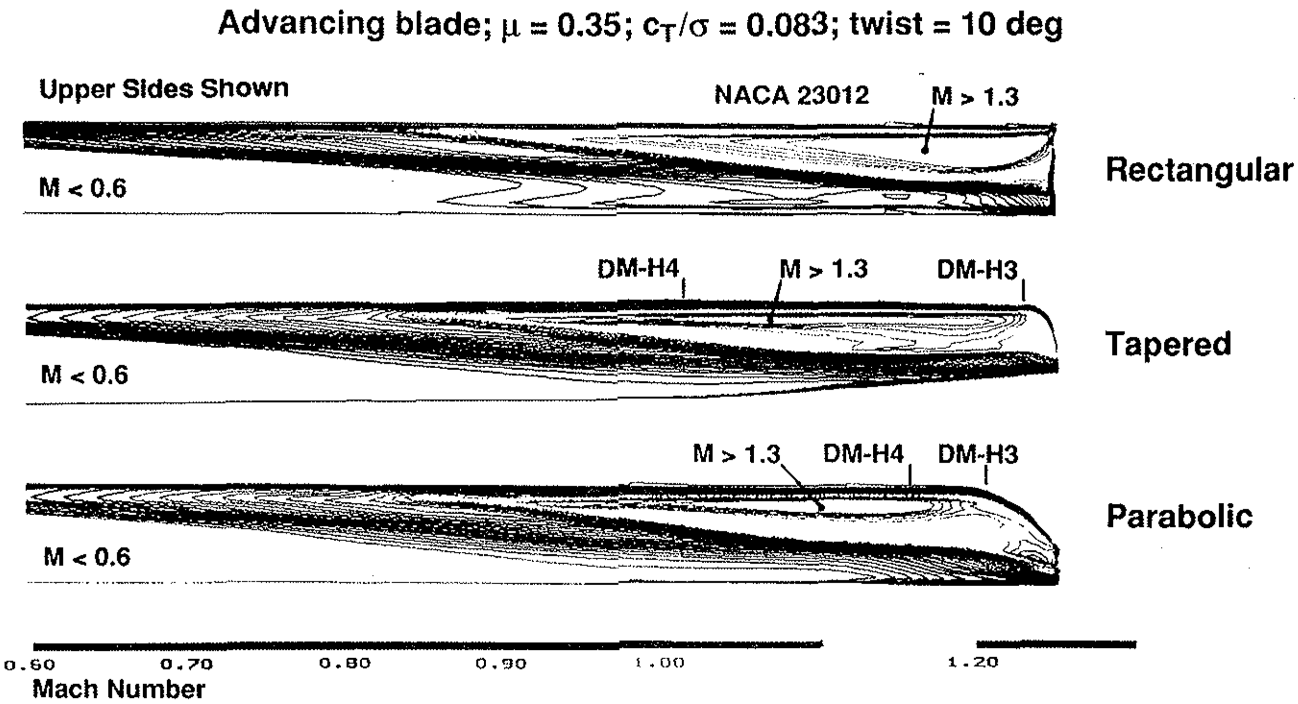

Fig.5: Reduction of transonic effects with advanced blade shape and airfoils

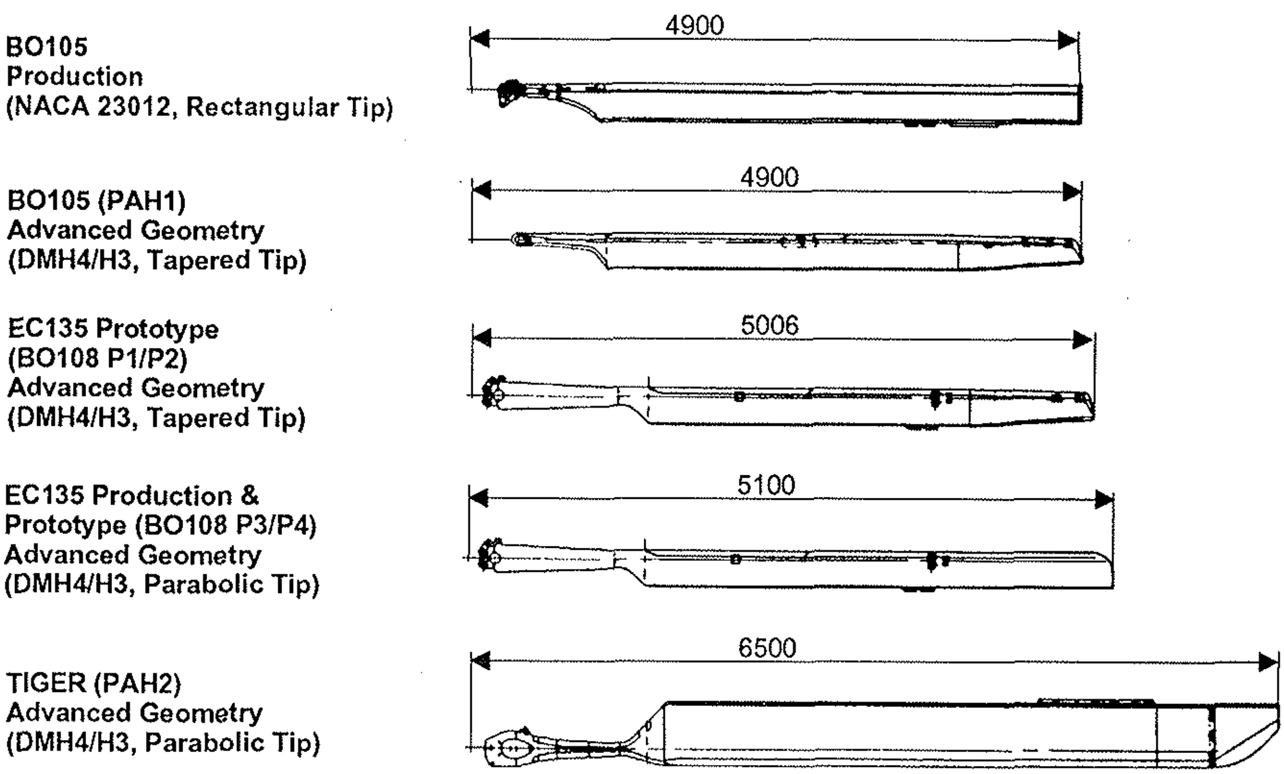

Fig.6: Rotor blade development at ECD

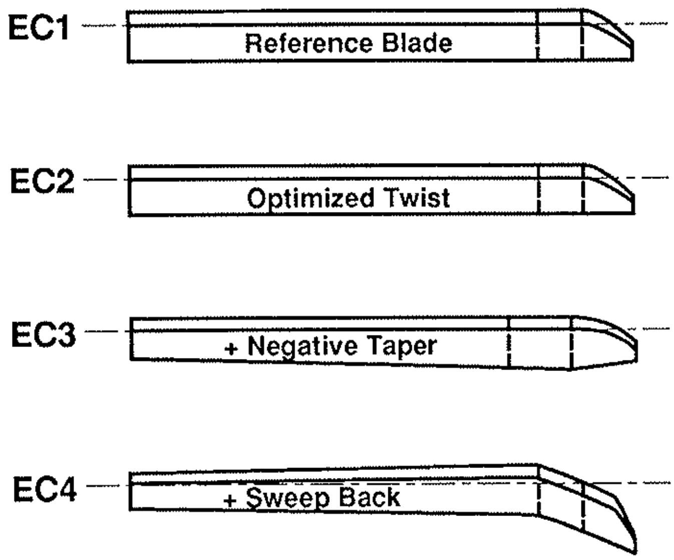

Performance Results (Model Rotor Wind Tunnel Test)		
	Lift/Drag	max. Thrust
EC1	reference	reference
EC2	-4%	+3%
EC3	+18%	+9%
EC4	+10%	+20%

*) at 350 km/h and $c_T/\sigma = 0.075$

**) at 150 km/h and $(c_p)_{Profile} = 0.0035$

Fig.7: Rotor research activities - ECD/ECF-Program ORPHEE

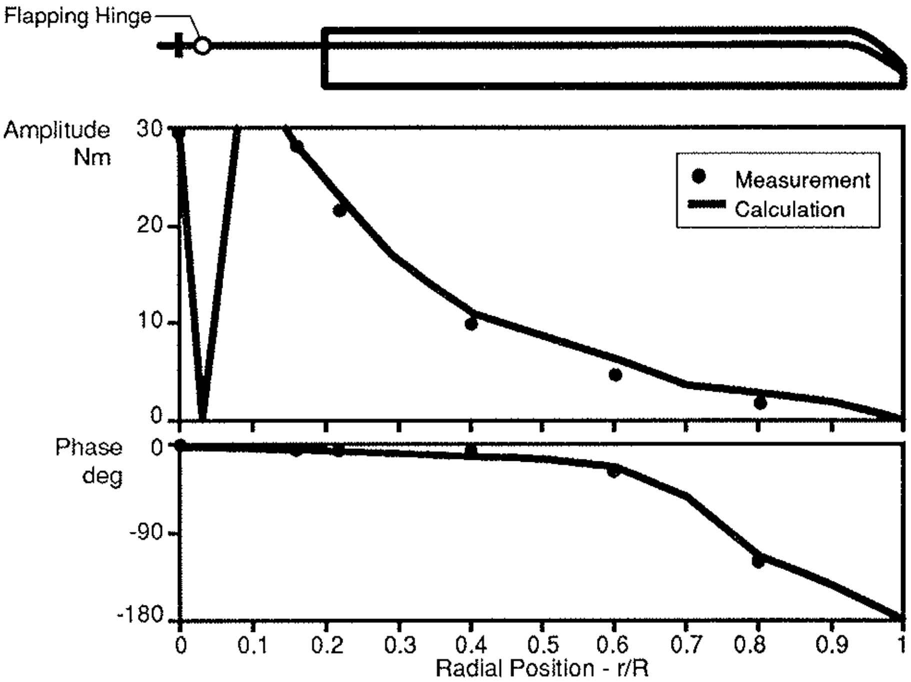

Program ORPHEE:
(Reference Blade EC1)

= 0.1

$\frac{c_T}{\ } = 0.075$

Fig.8: Aeroelastic blade loads - Calculation vs. WT-measurement
Radial distribution of 3/rev flap-bending moments

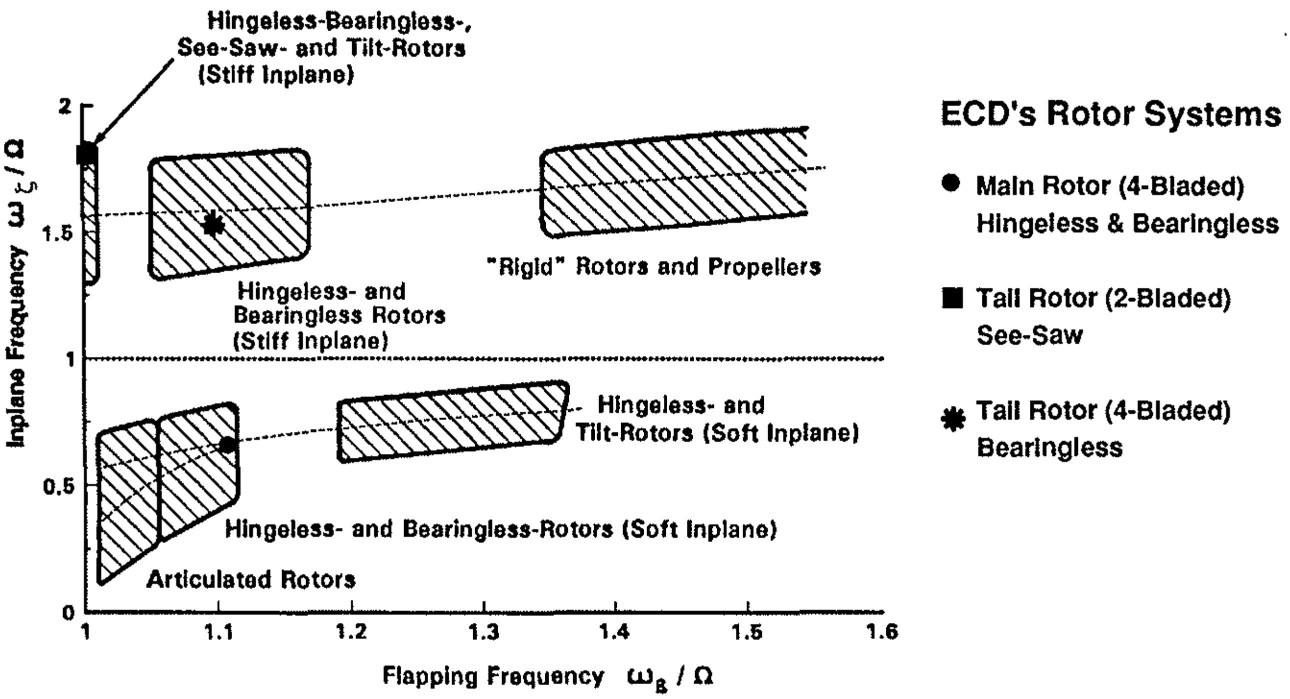

Fig.9: Dynamic layout of modern rotors - Fundamental flap-lag-frequency selection

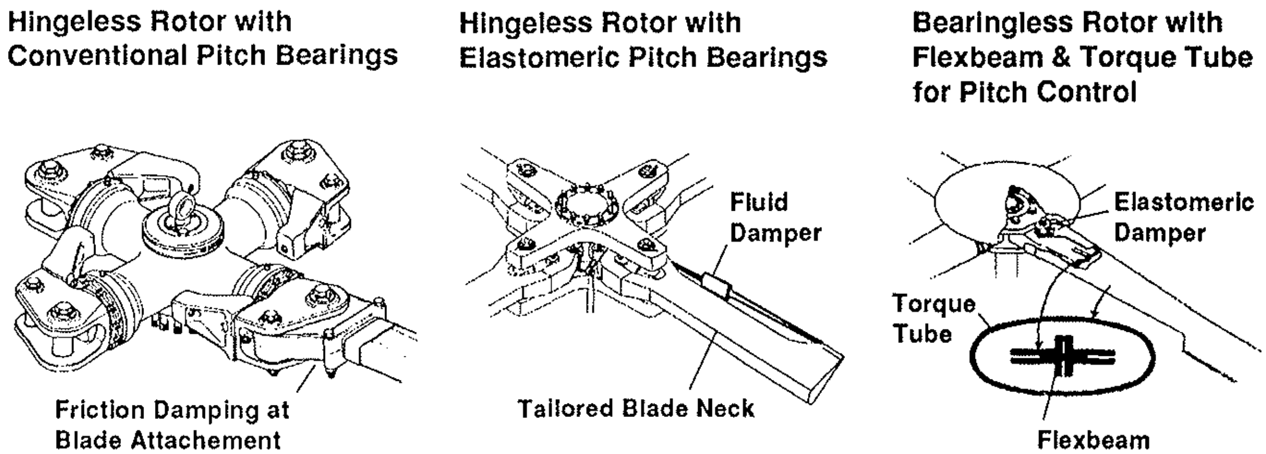

Fig.10: Lead-lag damping is a key item in the design of soft inplane rotor systems

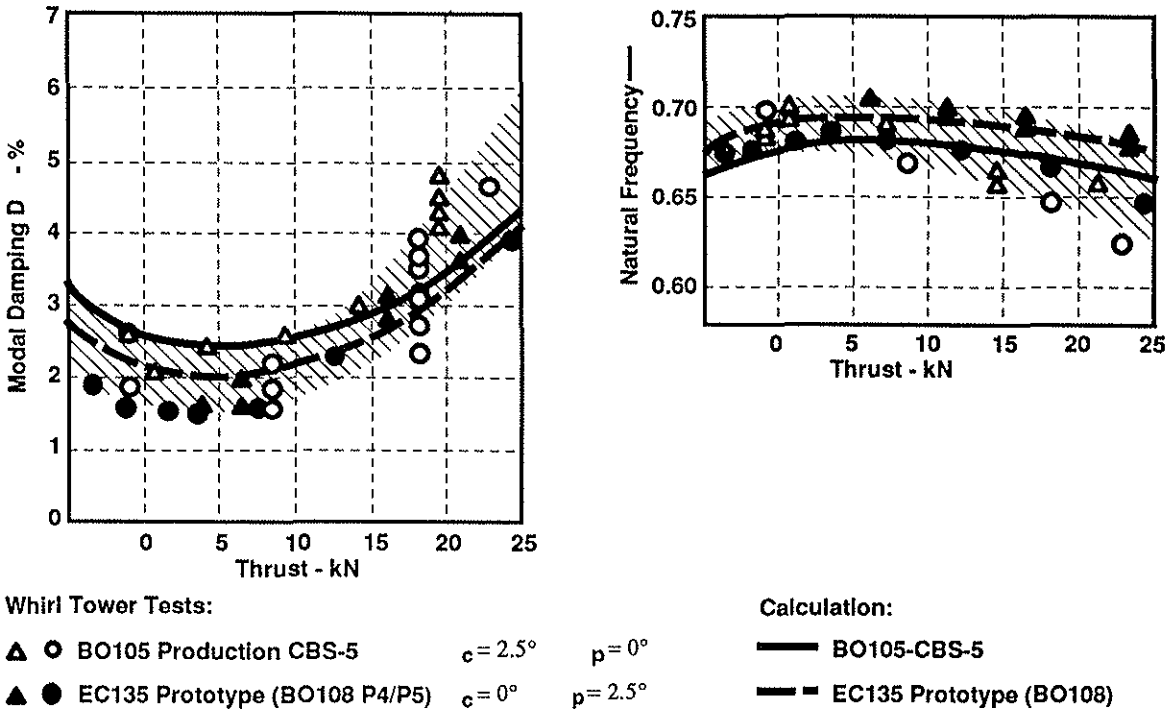

Fig.11: Aeroelastic blade coupling may improve rotor inplane damping

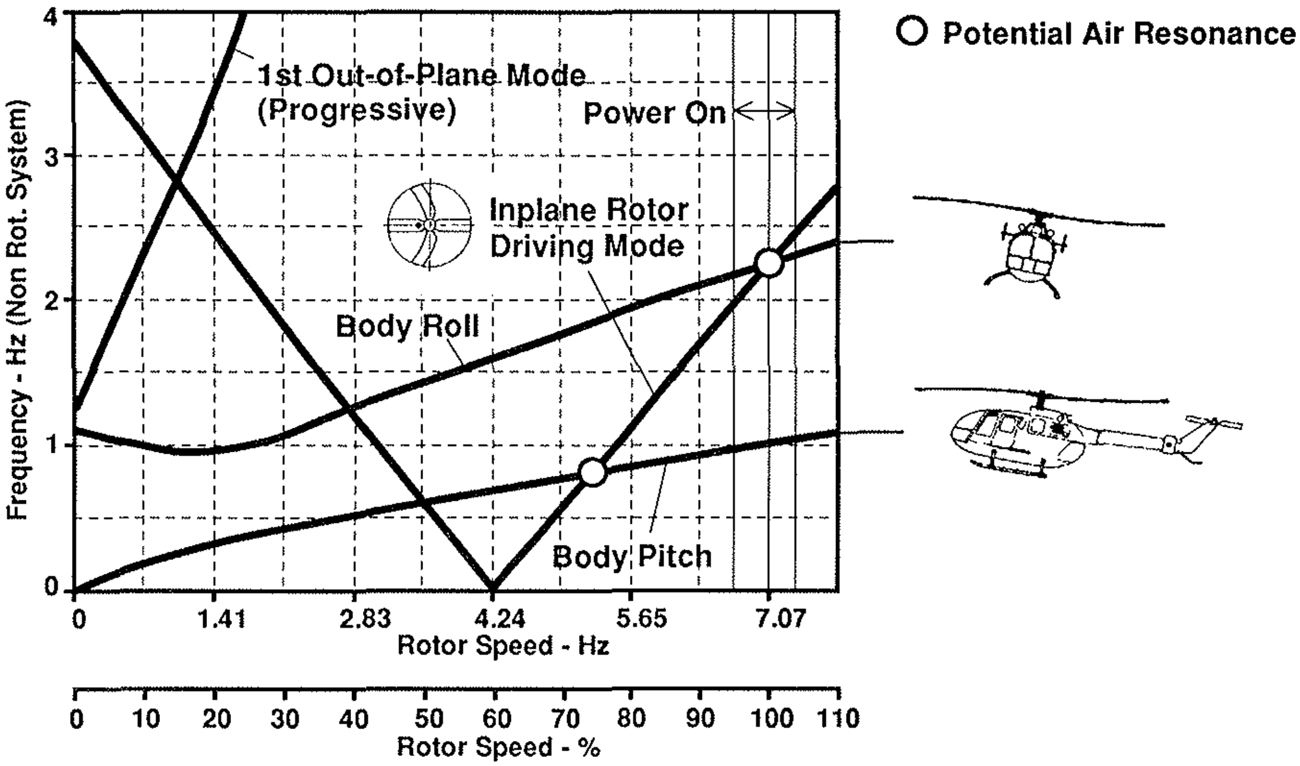

Fig.12: Air resonance frequency diagram (uncoupled modes)
Potential critical rotor speeds of BO105 CBS-5

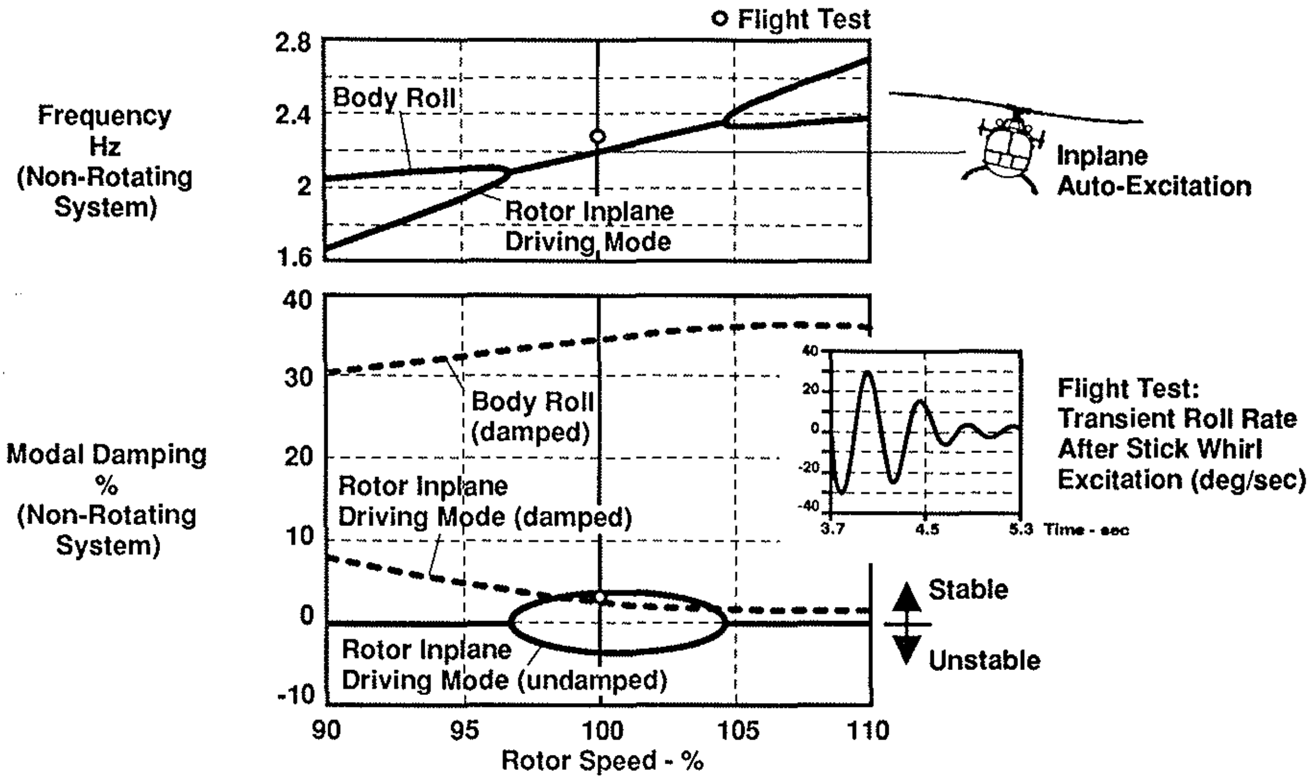

Fig.13: Rotor aerodynamics stabilize air resonance oscillations
BO105 CBS-5 at 60kts level flight

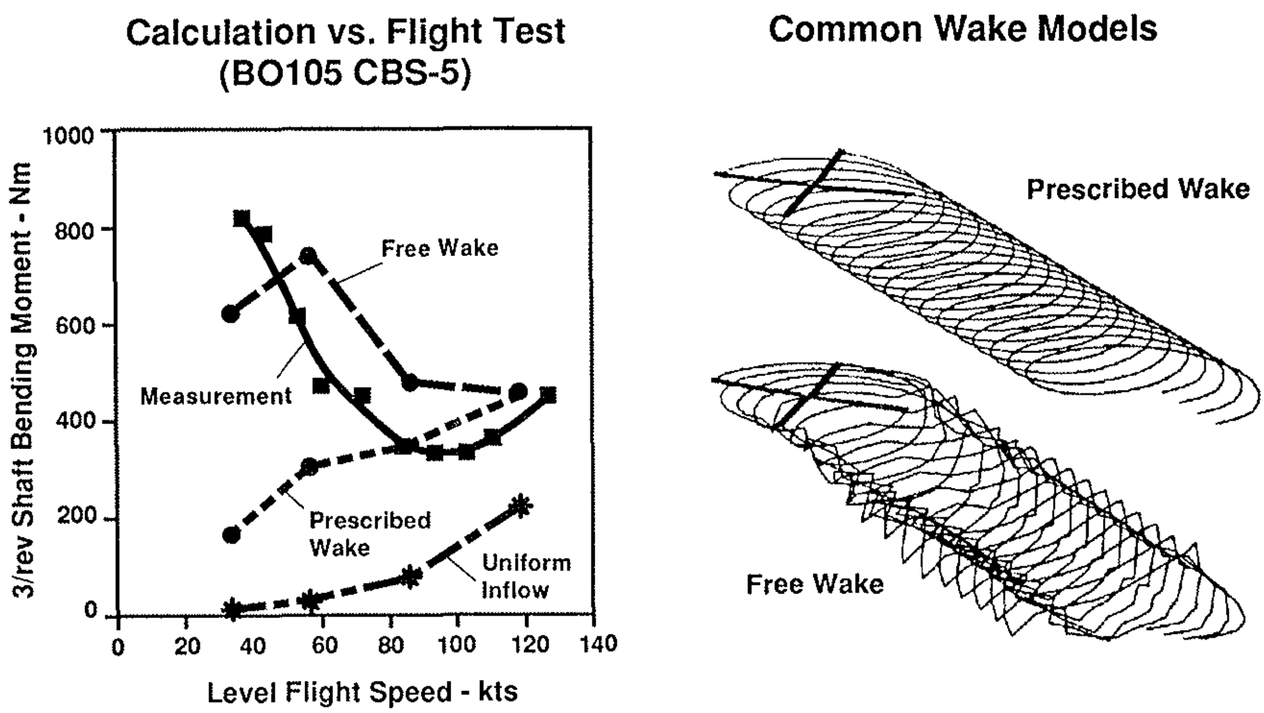

Fig.14: Vibratory hub load prediction requires adequate rotor wake models

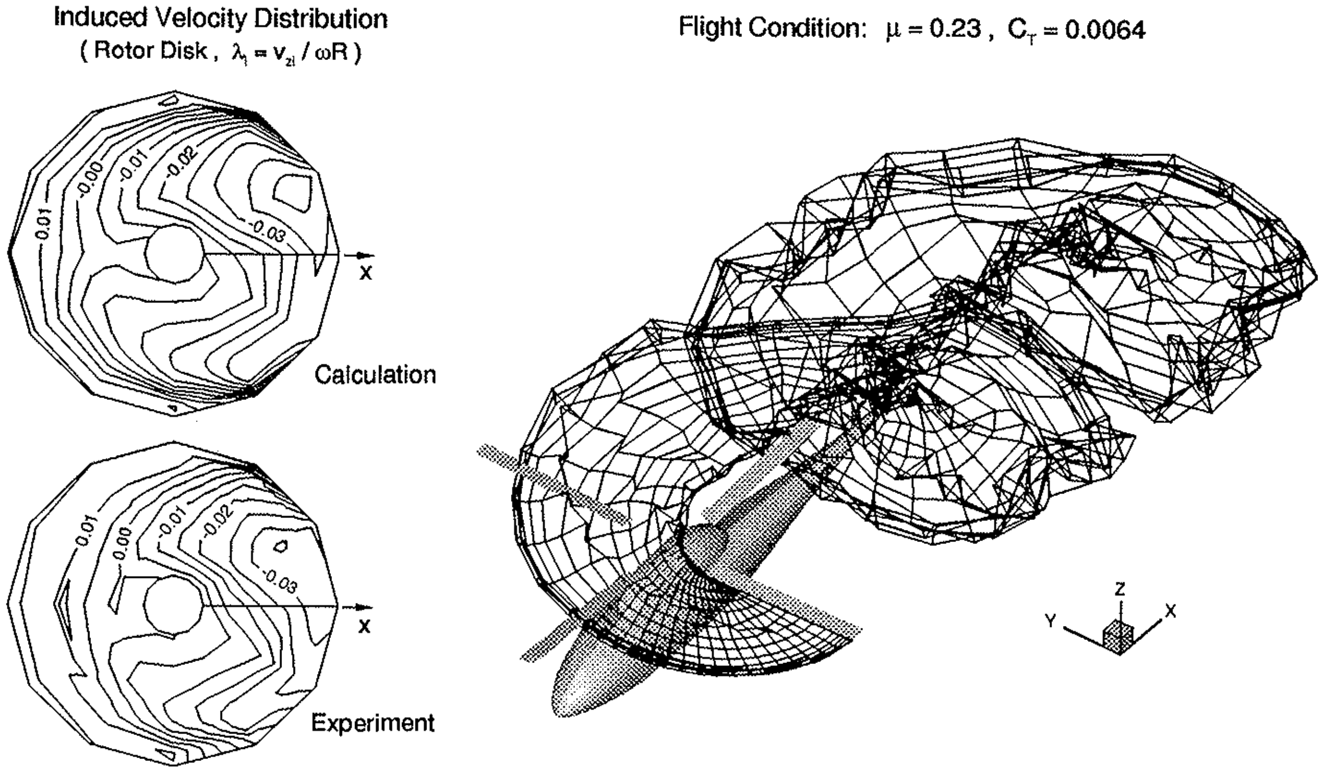

Fig.15: Rotor free wake simulation and resulting inflow at the rotor disk

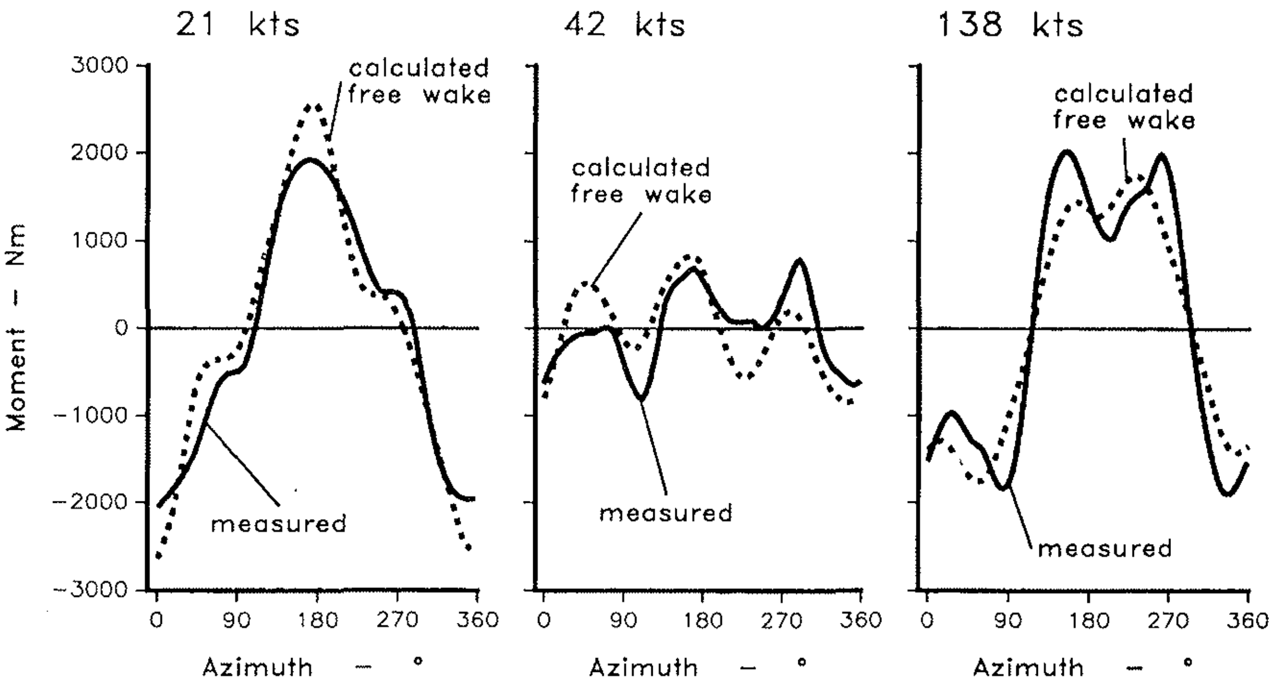

Fig.16: Prediction of rotor shaft bending moments by current aeroelastic tools
BO108 at level flight

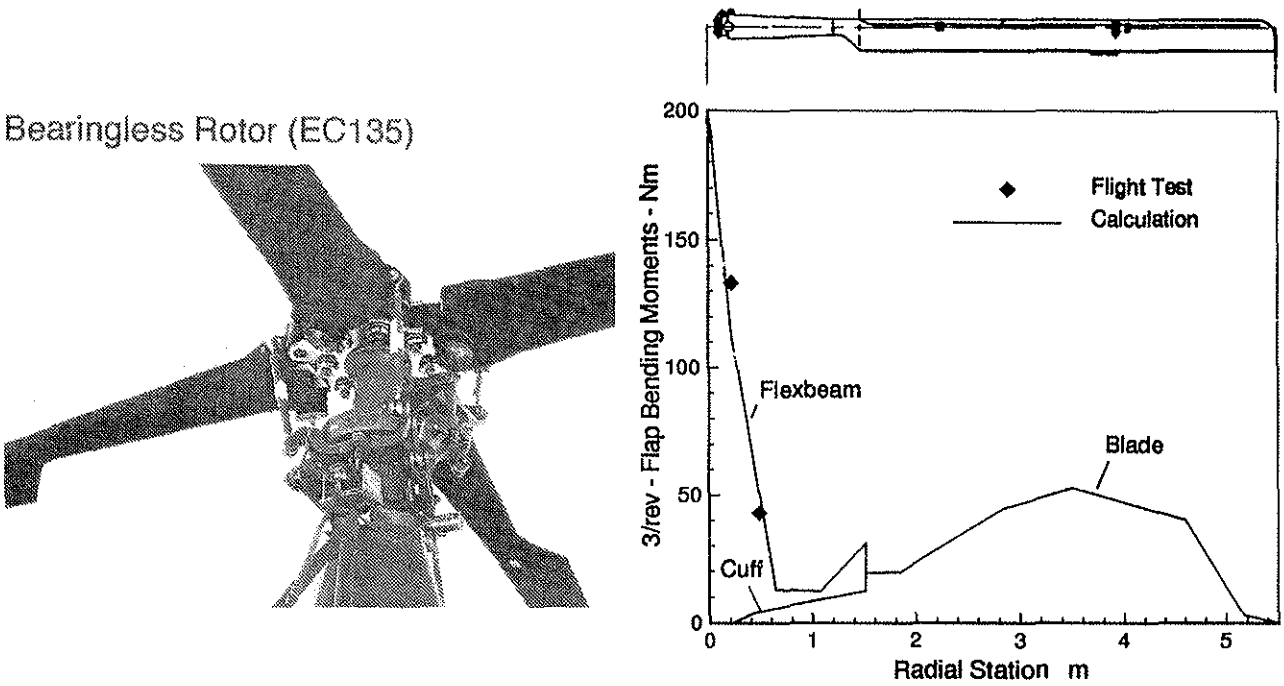

Fig.17: Bearingless rotor systems with redundant load paths require advanced modelling techniques
3/rev-blade flap-bending moments of EC135 at 32kts

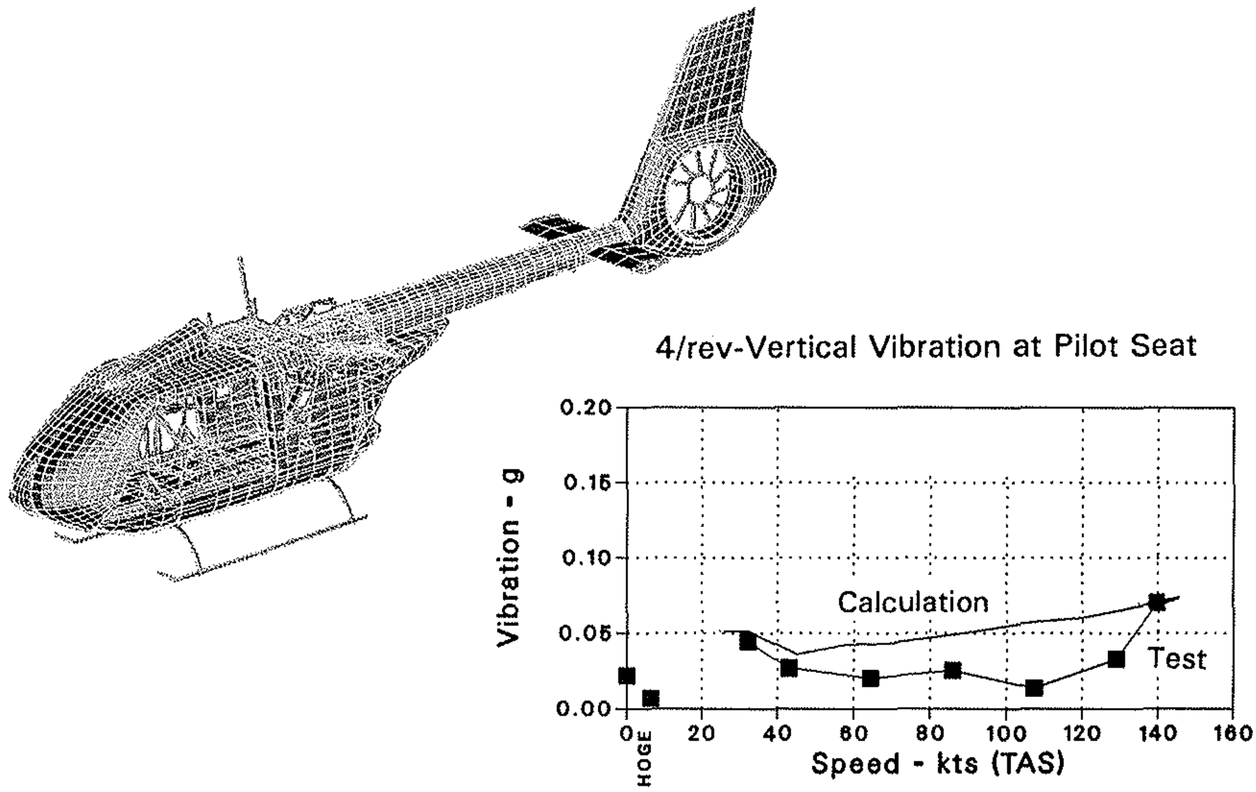

Fig.18: Helicopter airframe vibration prediction requires sophisticated dynamic and aerodynamic models
EC135 at level flight

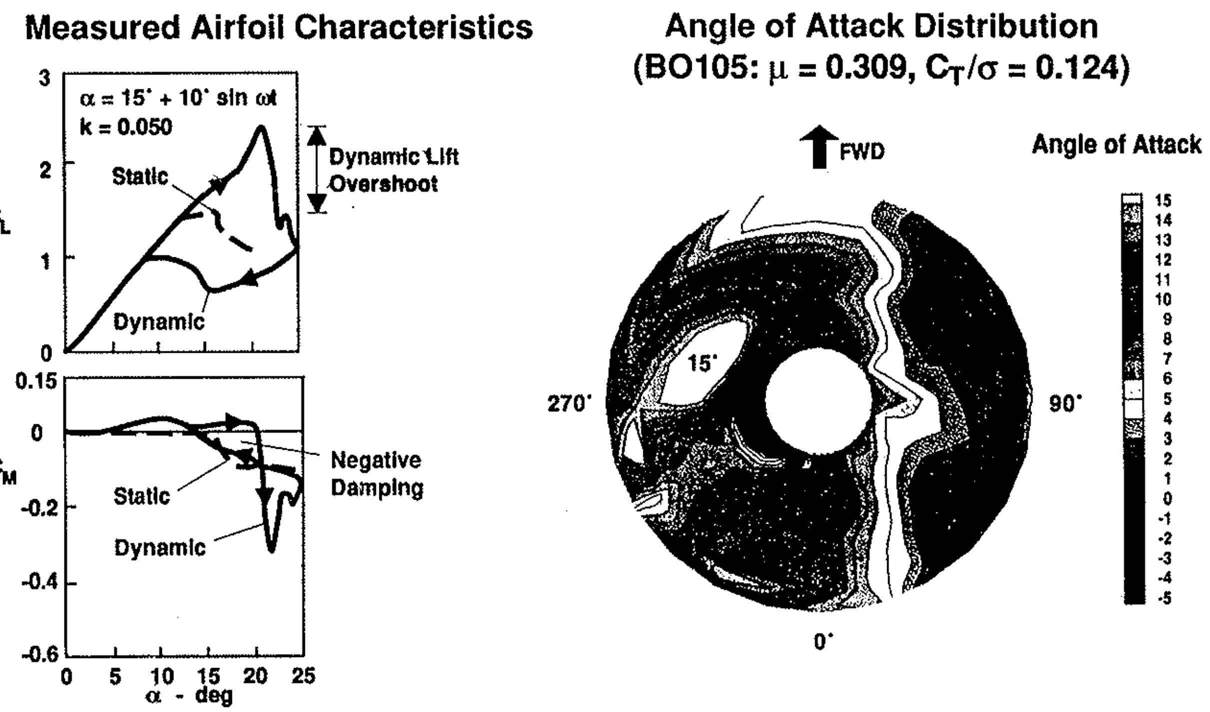

Fig.19: Dynamic stall effects are a key for high speed rotor load prediction

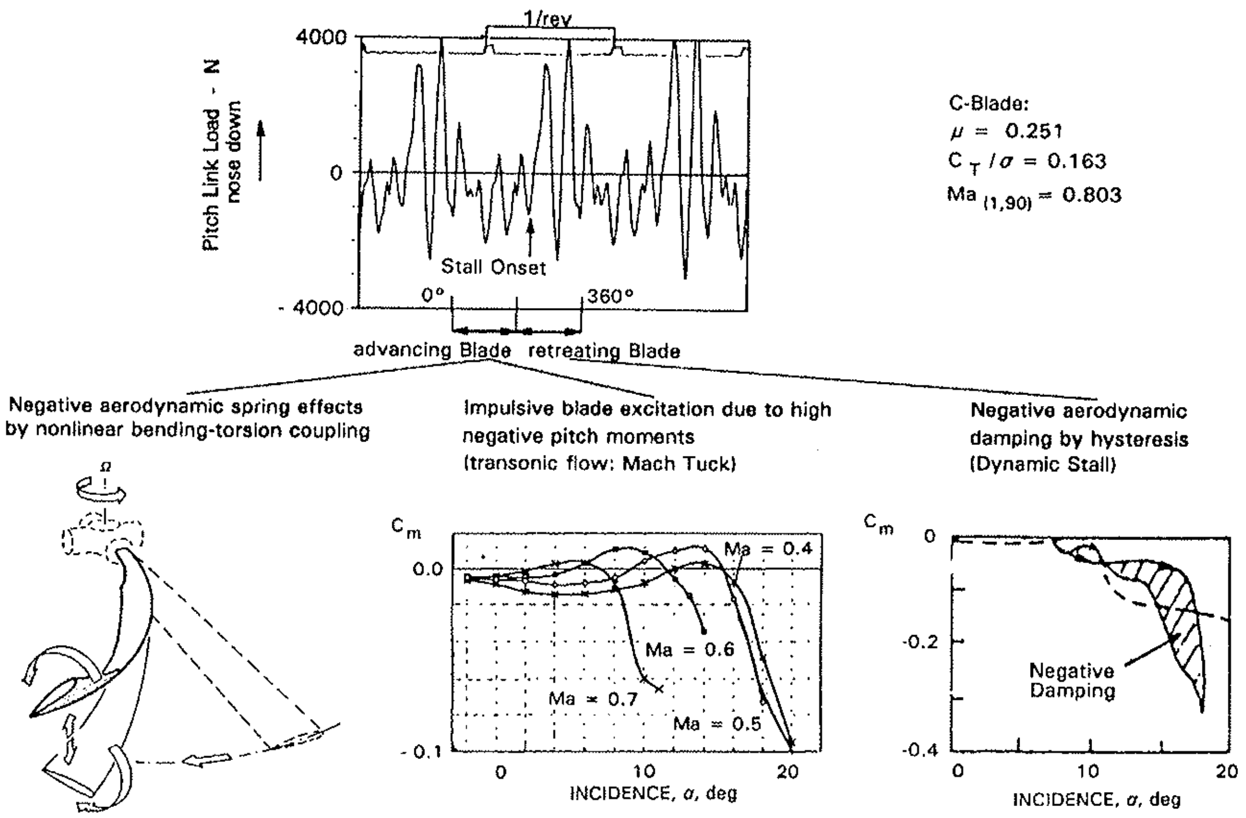

Fig.20: Torsional excitation of a rotor blade during high g - manoeuvers

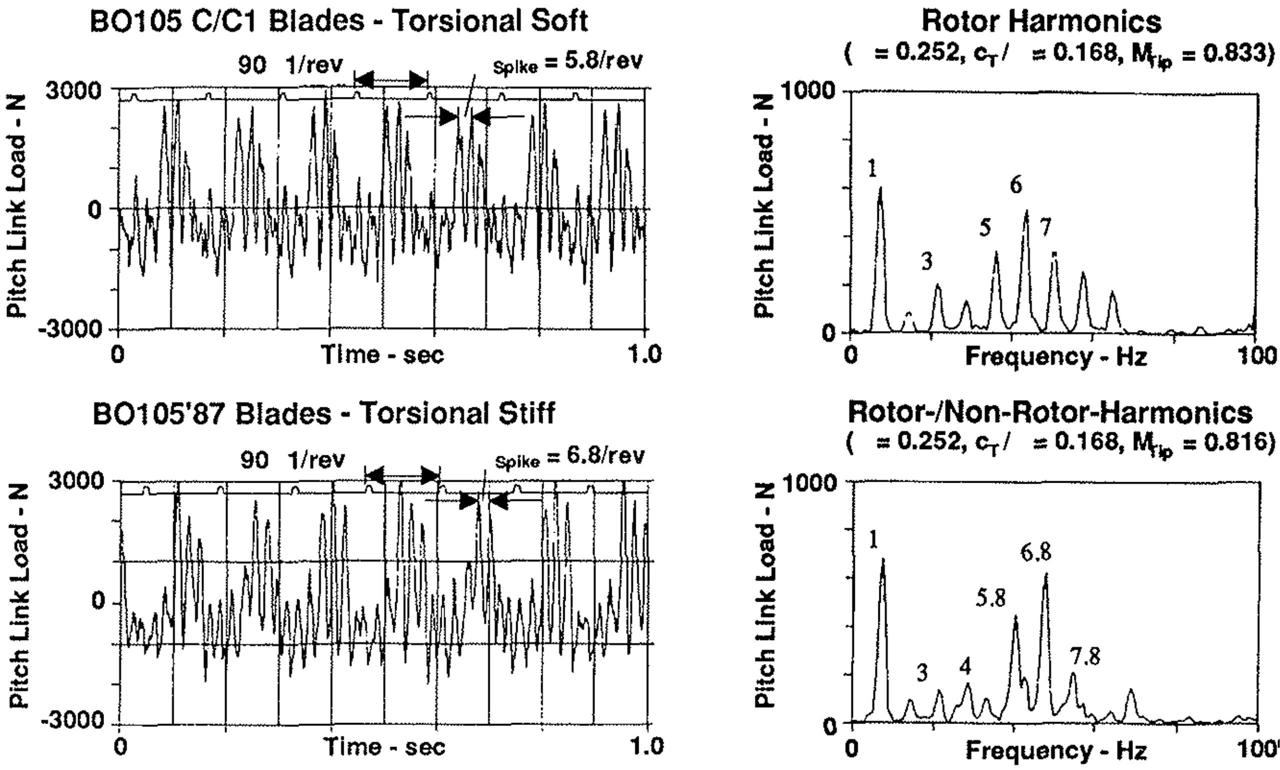

Fig.21: Pitch link load oscillations of advanced geometry blades at deep stall conditions
BO105 flight tests (turns) with

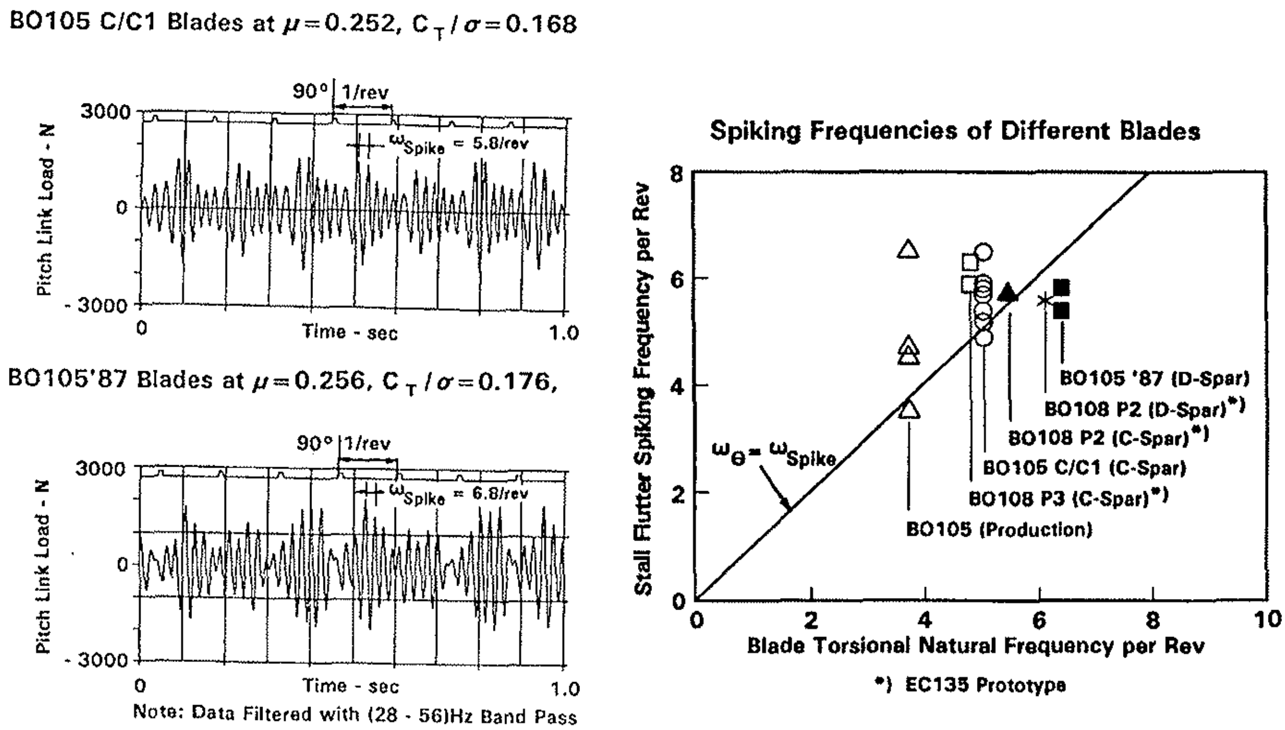

Fig.22: Stall flutter is accompanied by high frequency pitch link oscillations (flight test results)

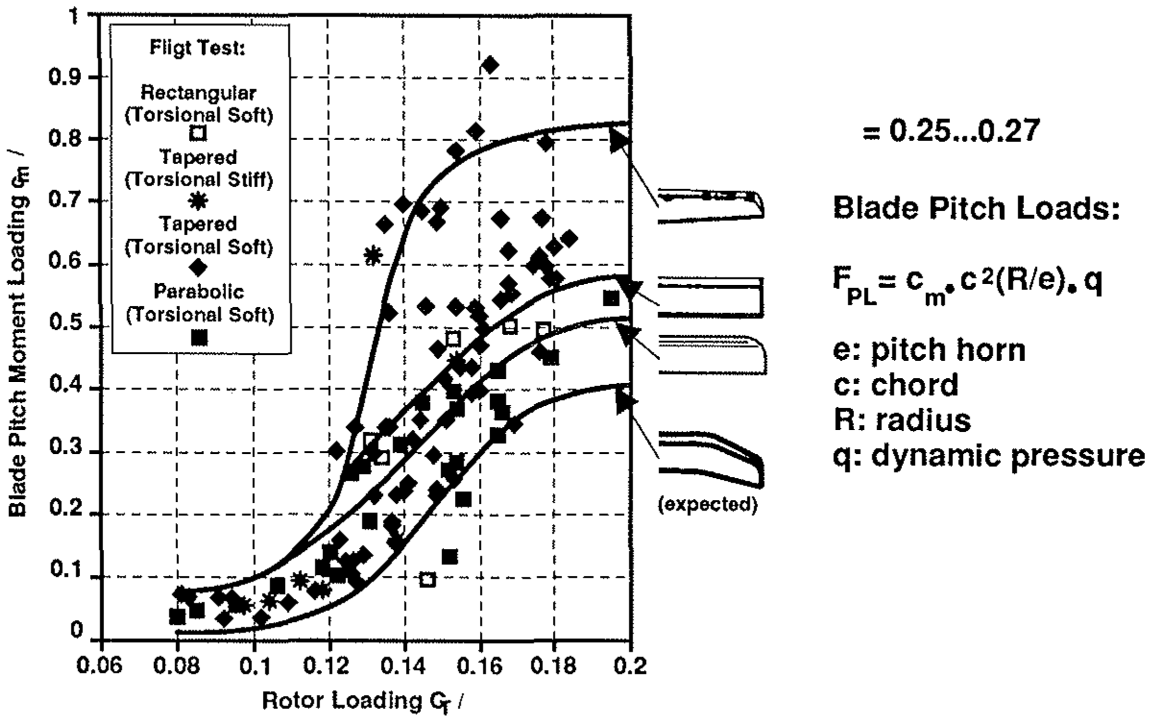

Fig.23: Reduction of stall flutter induced pitch link loads by blade tip design

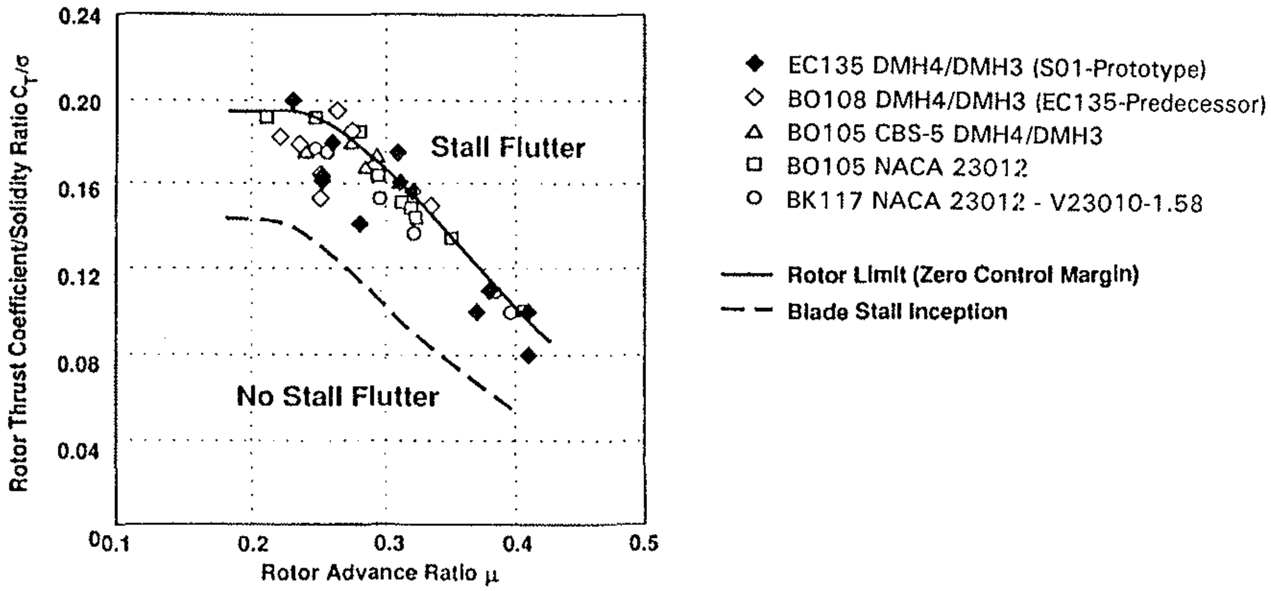

Fig.24: Rotor stall flutter boundaries - Flight test results

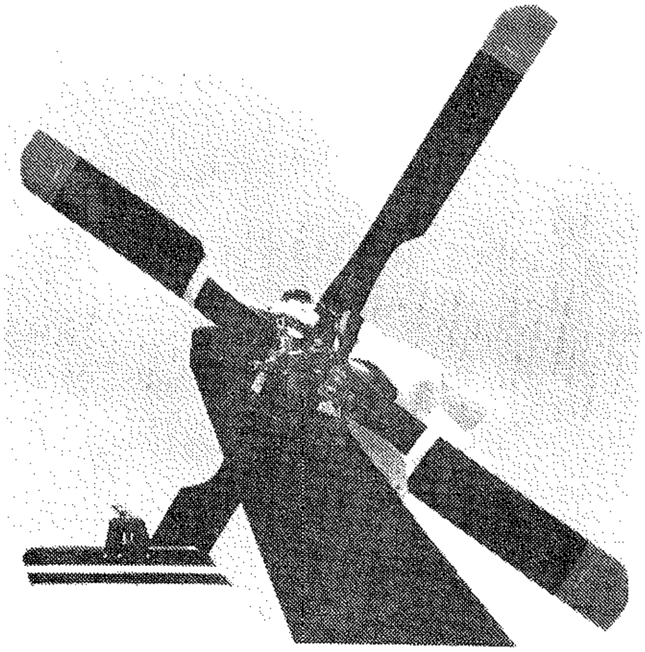

Fig.25: Stiff inplane bearingless tail rotor (ALH-BTR)

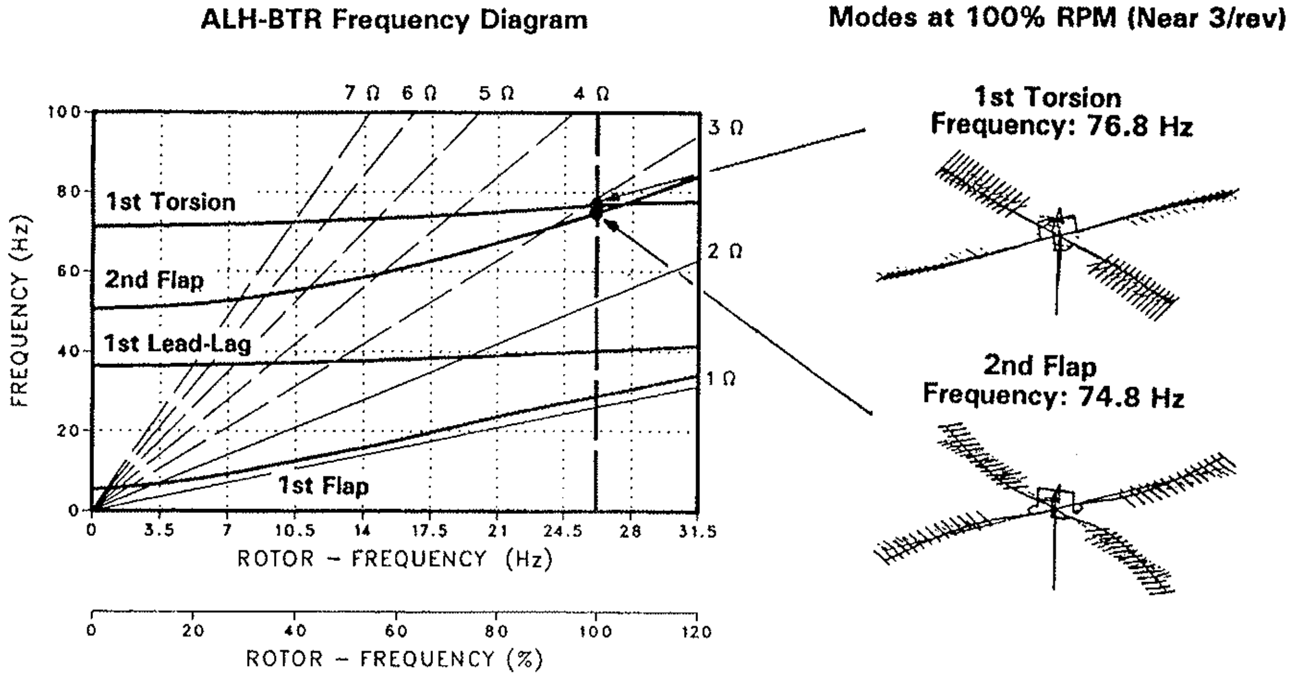

Fig.26: Bearingless tail-rotor dynamics - Cyclic modes of ALH-BTR

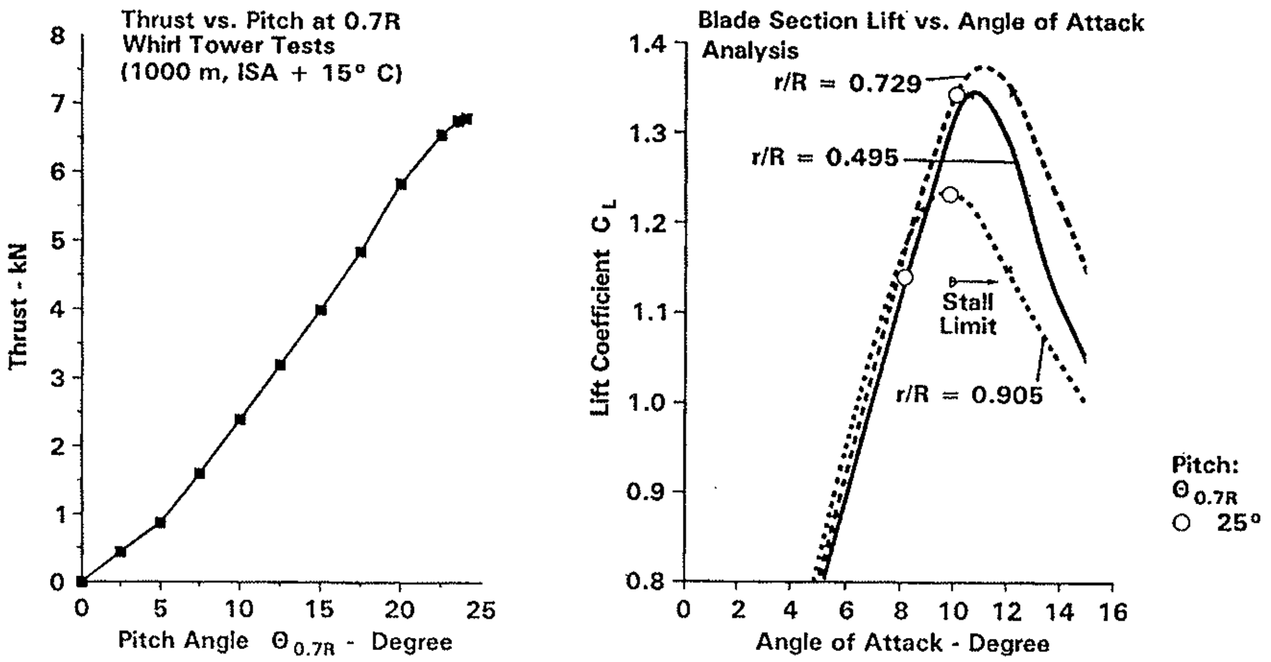

Fig.27: Tail rotor thrust potential of ALH-BTR

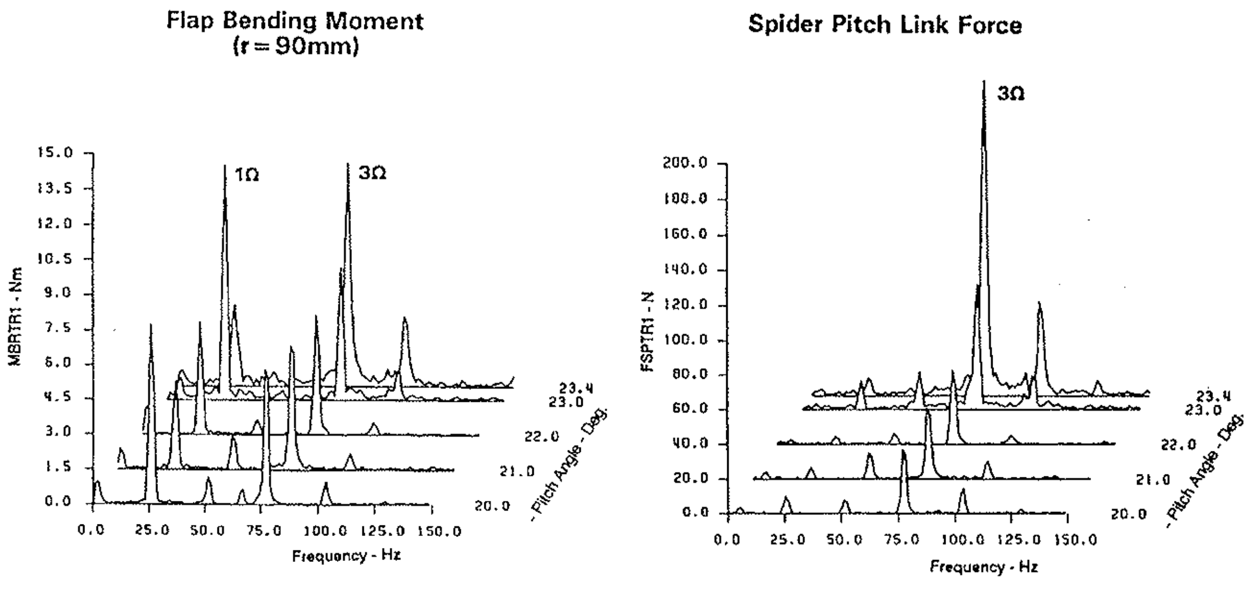

Fig.28: Whirl tower testing of the ALH-BTR at high thrust and 100% rpm
Ampliude spectra at pitch angles just below stall induced limit cycle oscillations

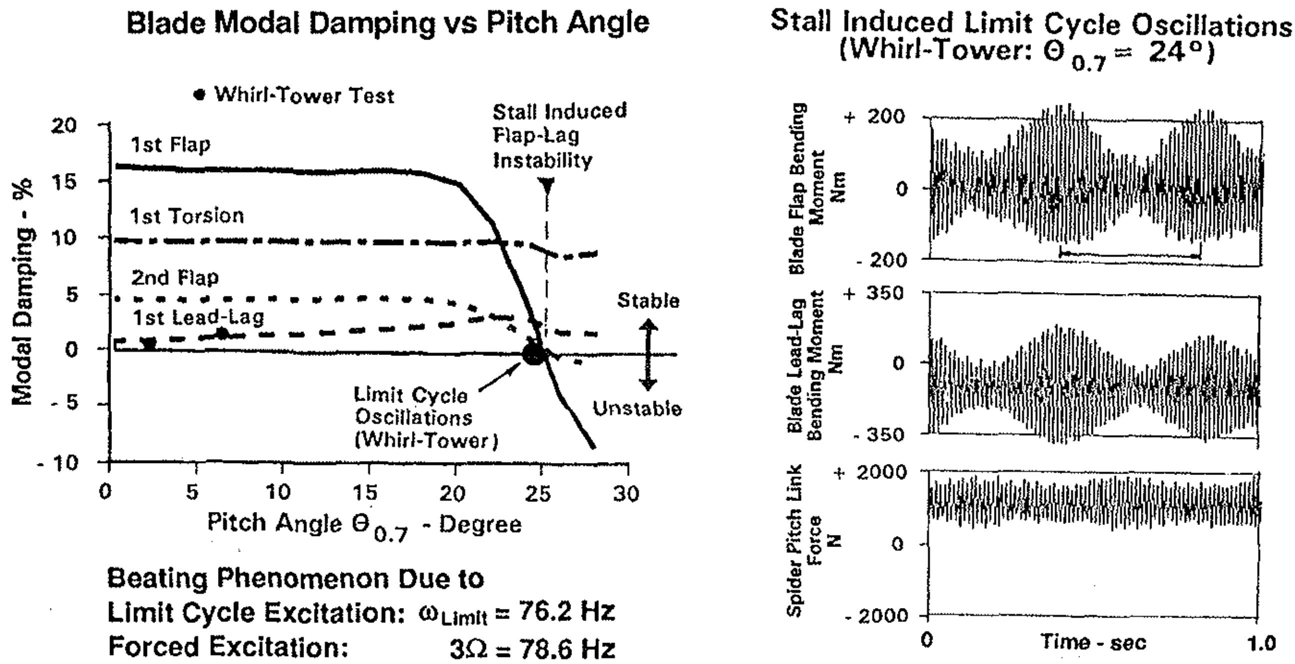

Fig.29: Tail rotor operational range limited by stall induced flap-lag-torsion blade instability

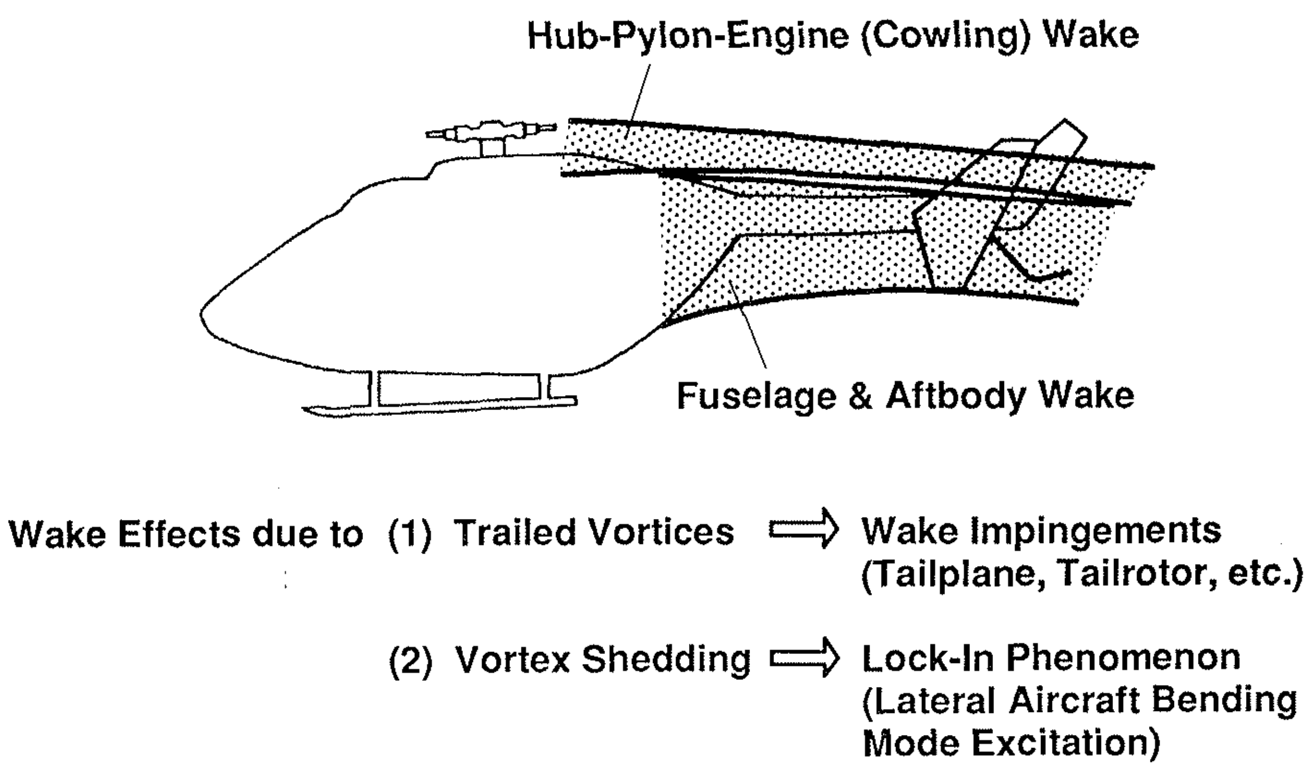

Fig.30: Helicopter tail shake explained by interactional aerodynamic effects

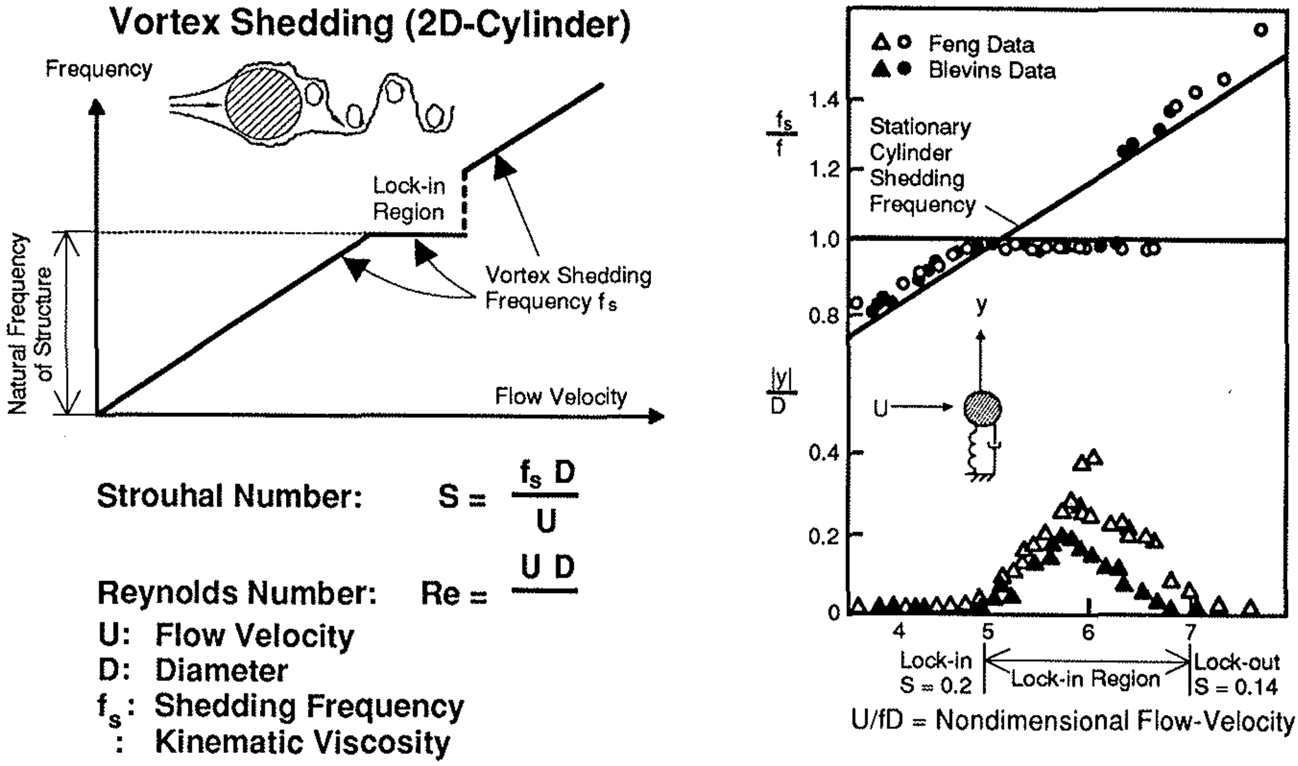

Fig.31: Influence of vortex-shedding on structural dynamics - the lock-in phenomenon

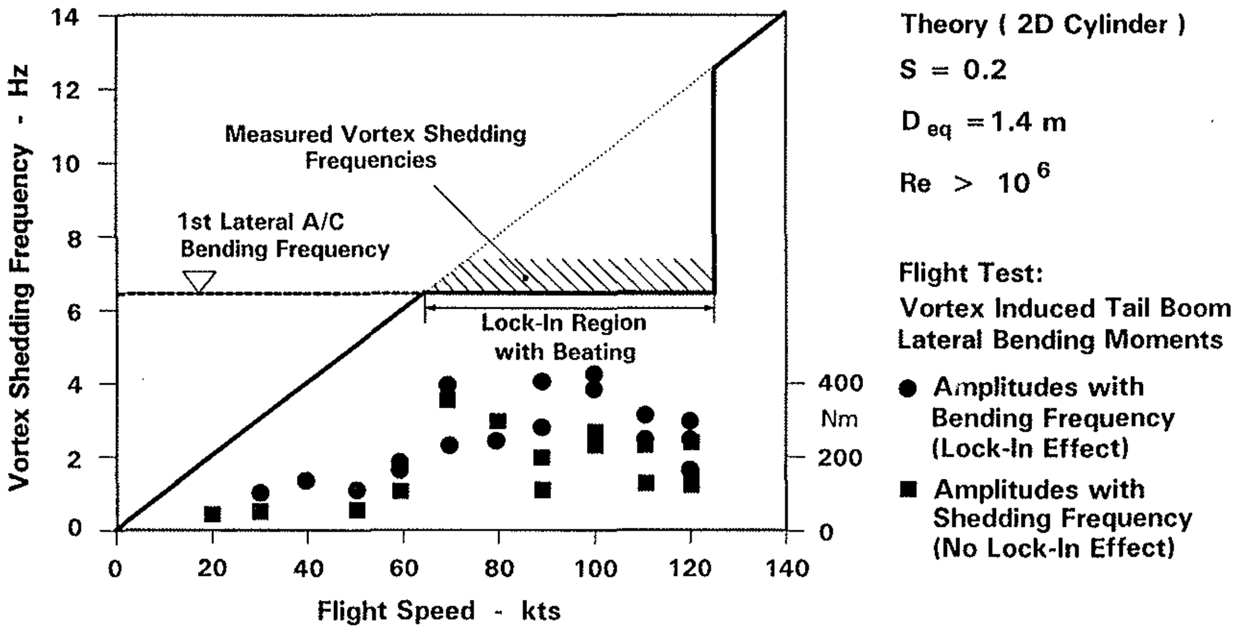

Fig.32: BK117 tail shake explained by the lock-in phenomenon

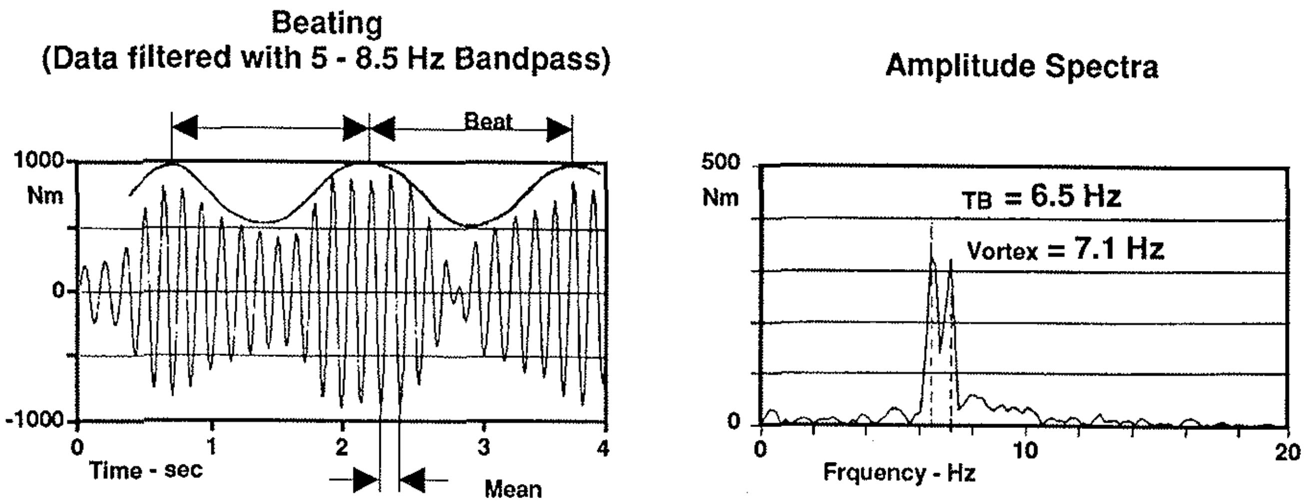

Interpretation of measured frequencies:

Beat = Vortex - TB	TB	: Bending frequency (Lock-in)
Mean = 1/2 (Vortex + TB)	Vortex	: Shedding frequency

Fig.33: Beating by tail shake – Lateral tail boom bending moments
BK117 at 70kts, 500ft/min, ROD

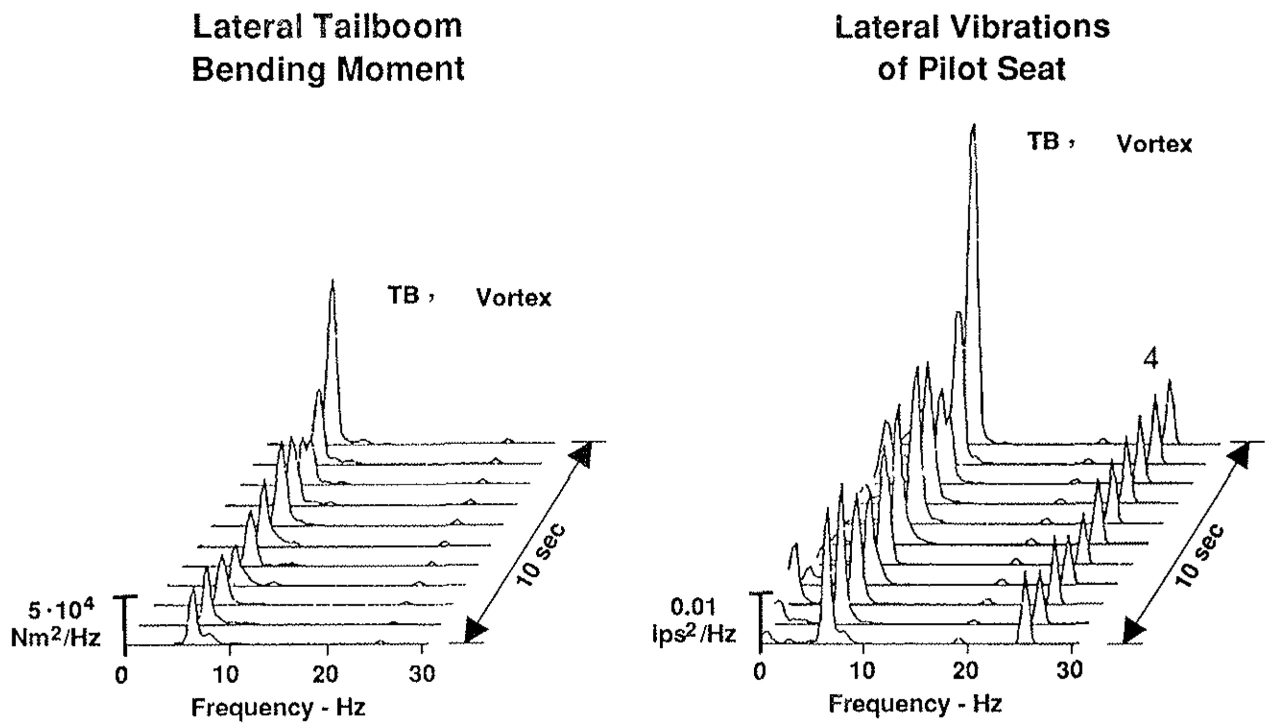

Fig.34: Tail shake excitation study – Power spectra measurements
BK117 at 70kts, 500ft/min ROD

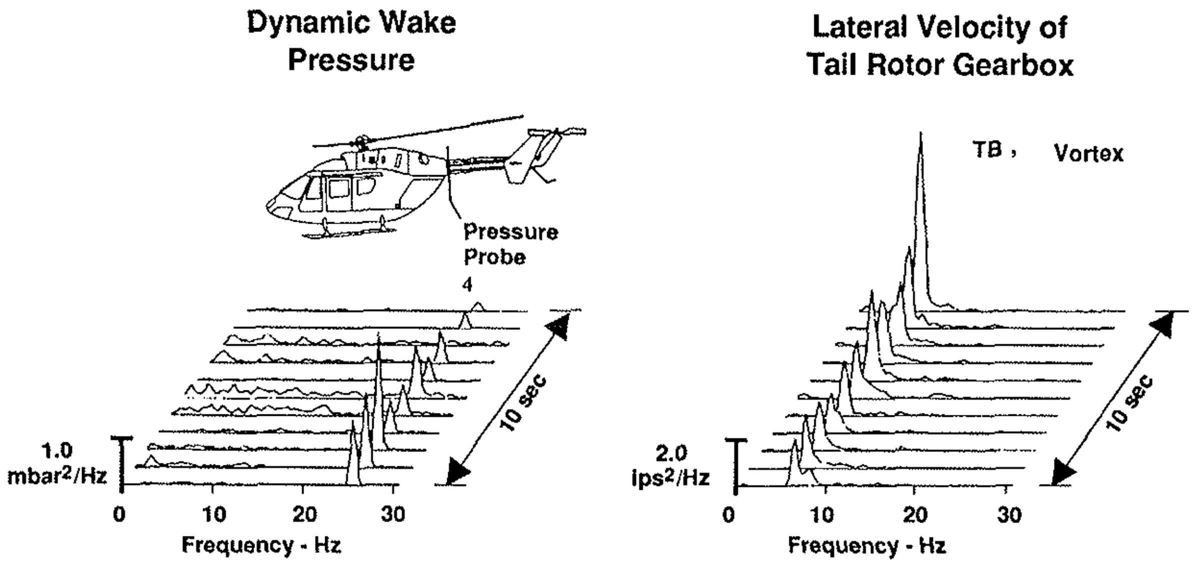

Fig.35: Tail shake excitation by wake impingement not measured in power spectra
BK117 at 70kts, 500ft/min ROD

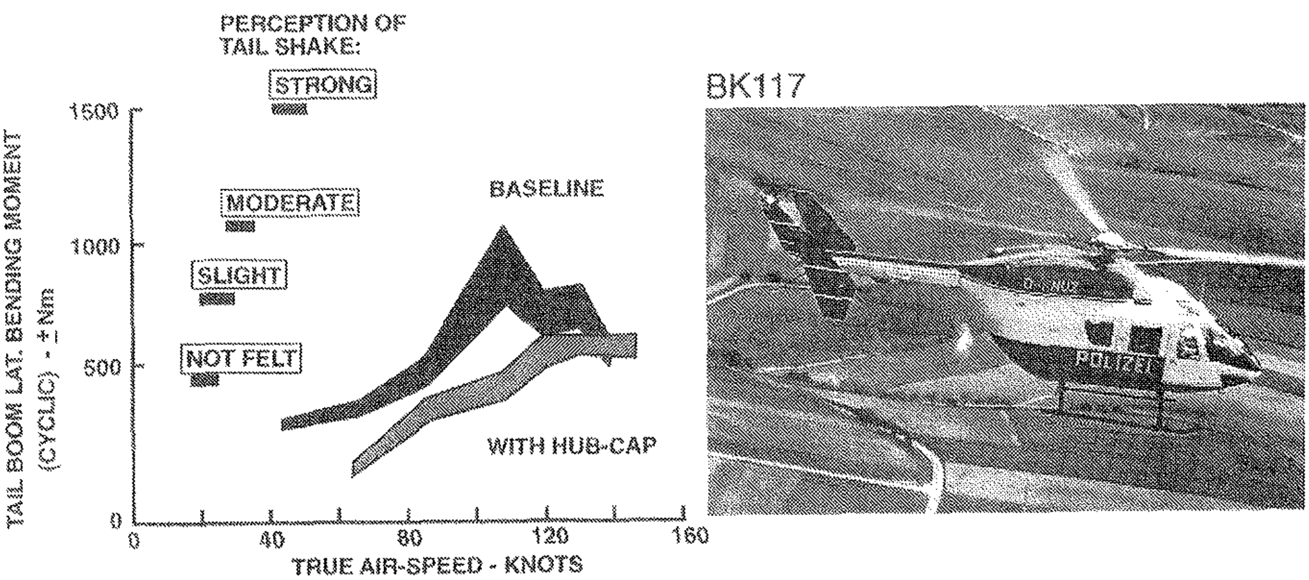

Fig.36: Hub cap improves tail shake (BK117 flight test results)

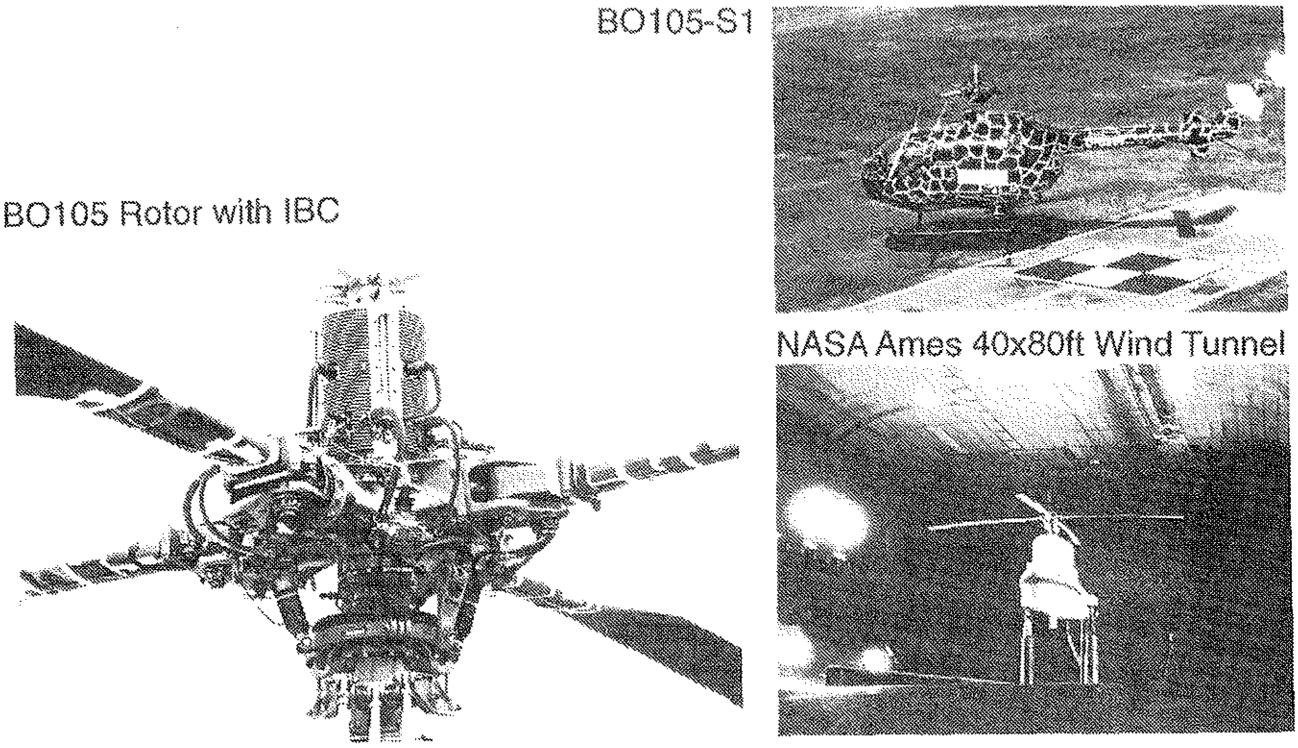

Fig.37: Individual blade control research activities on BO105

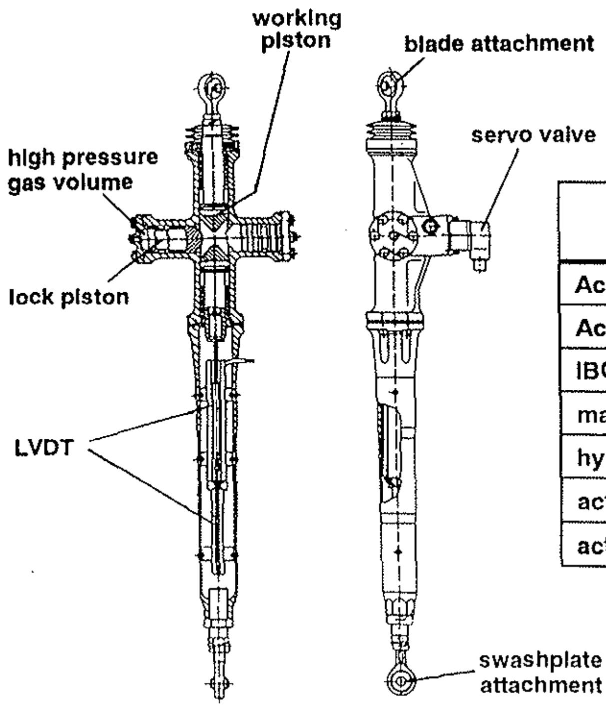

	Flight test	Wind tunnel test
Actuator length	289 mm	682 mm
Actuator stroke	1.5 mm	9 mm
IBC blade pitch	0.42 deg.	3 deg.
max. frequency	35 Hz	42 (64) Hz
hydr. pressure	207 bar	207 bar
actuator force	2000 N	5000 N
actuator mass	2.5 kg	5.0 kg

Fig.38: IBC-actuator for full scale testing on BO105

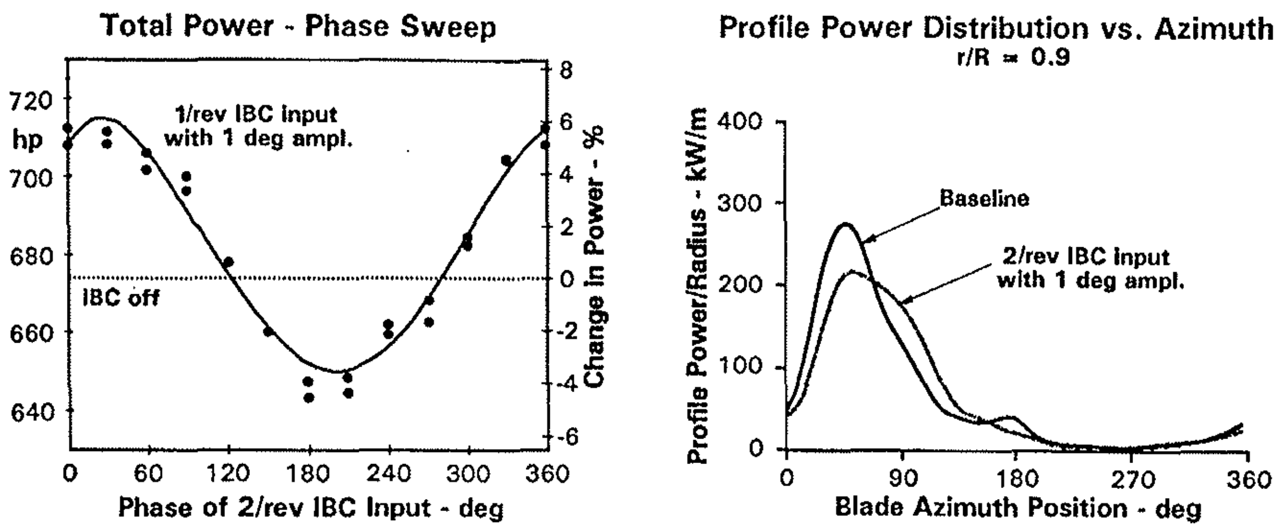

Fig.39: Power reduction by 2/rev-blade pitch inputs – BO105 full scale wind tunnel tests

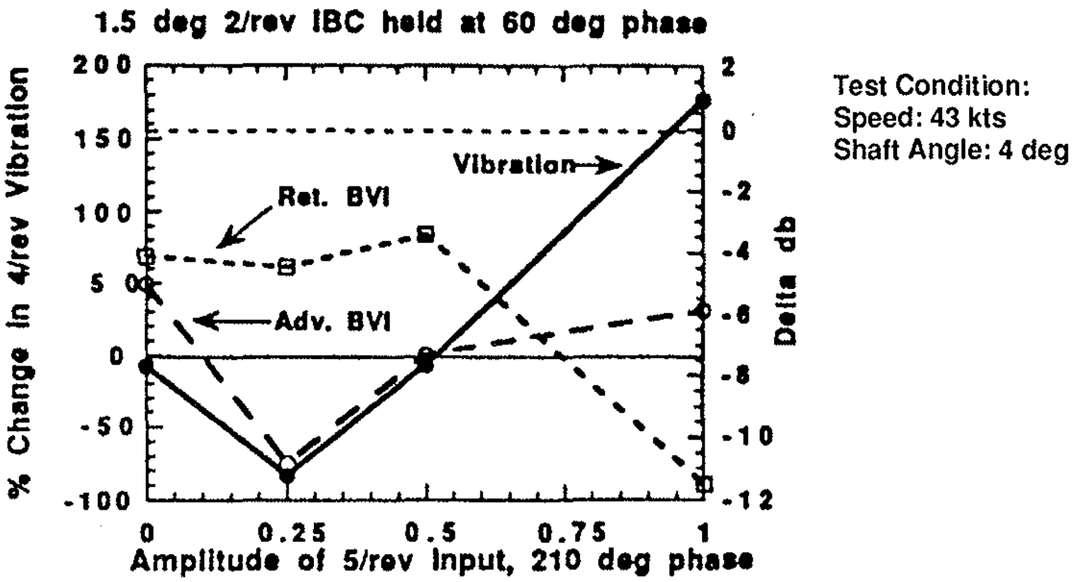

Fig.40: Simultaneous vibration and noise reduction by IBC – BO105 full scale wind tunnel tests

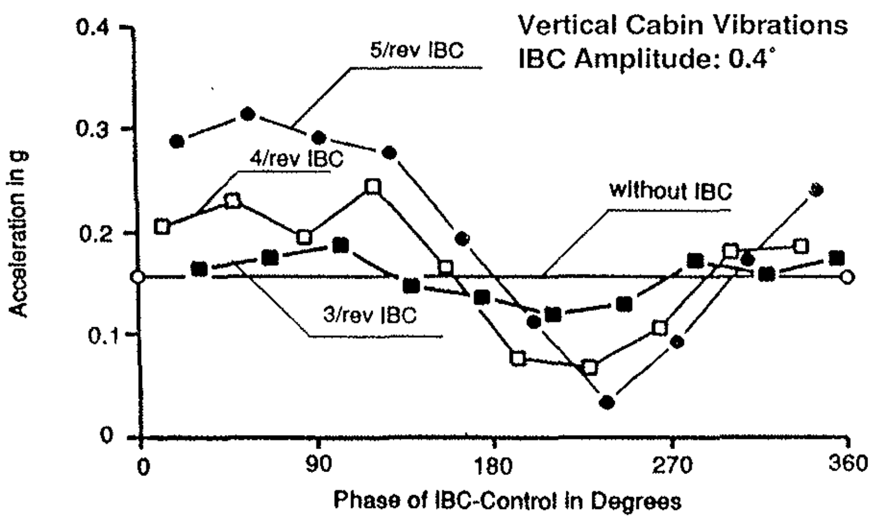

Fig.41: 4/rev vibration control by IBC – BO105 level flight tests ($\mu = 0.14$)